



**DISCRETE AND CONTINUOUS MODELS
AND APPLIED COMPUTATIONAL
SCIENCE**

Volume 30 Number 4 (2022)

Founded in 1993

Founder: PEOPLES' FRIENDSHIP UNIVERSITY OF RUSSIA

DOI: 10.22363/2658-4670-2022-30-4

Edition registered by the Federal Service for Supervision of Communications,
Information Technology and Mass Media
Registration Certificate: ПИ № ФС 77-76317, 19.07.2019

ISSN 2658-7149 (online); 2658-4670 (print)
4 issues per year.
Language: English.

Publisher: Peoples' Friendship University of Russia (RUDN University).
Indexed by Ulrich's Periodicals Directory (<http://www.ulrichsweb.com>),
Directory of Open Access Journals (DOAJ) (<https://doaj.org/>), Russian
Index of Science Citation (<https://elibrary.ru>), EBSCOhost (<https://www.ebsco.com>), CyberLeninka (<https://cyberleninka.ru>).

Aim and Scope

Discrete and Continuous Models and Applied Computational Science arose in 2019 as a continuation of RUDN Journal of Mathematics, Information Sciences and Physics. RUDN Journal of Mathematics, Information Sciences and Physics arose in 2006 as a merger and continuation of the series "Physics", "Mathematics", "Applied Mathematics and Computer Science", "Applied Mathematics and Computer Mathematics".

Discussed issues affecting modern problems of physics, mathematics, queuing theory, the Teletraffic theory, computer science, software and databases development.

It's an international journal regarding both the editorial board and contributing authors as well as research and topics of publications. Its authors are leading researchers possessing PhD and PhDr degrees, and PhD and MA students from Russia and abroad. Articles are indexed in the Russian and foreign databases. Each paper is reviewed by at least two reviewers, the composition of which includes PhDs, are well known in their circles. Author's part of the magazine includes both young scientists, graduate students and talented students, who publish their works, and famous giants of world science.

The Journal is published in accordance with the policies of COPE (Committee on Publication Ethics). The editors are open to thematic issue initiatives with guest editors. Further information regarding notes for contributors, subscription, and back volumes is available at <http://journals.rudn.ru/miph>.

E-mail: miphj@rudn.ru, dcm@sci.pfu.edu.ru.

EDITORIAL BOARD

Editor-in-Chief

Yury P. Rybakov, Doctor of Sciences in Physics and Mathematics, Professor, Honored Scientist of Russia, Professor of the Institute of Physical Research & Technologies, Peoples' Friendship University of Russia (RUDN University), Moscow, Russian Federation

Vice Editors-in-Chief

Leonid A. Sevastianov, Doctor of Sciences in Physics and Mathematics, Professor, Professor of the Department of Applied Probability and Informatics, Peoples' Friendship University of Russia (RUDN University), Moscow, Russian Federation

Dmitry S. Kulyabov, Doctor of Sciences in Physics and Mathematics, Docent, Professor of the Department of Applied Probability and Informatics, Peoples' Friendship University of Russia (RUDN University), Moscow, Russian Federation

Members of the editorial board

Konstantin E. Samouylov, Doctor of Sciences in Technical Sciences, Professor, Head of Department of Applied Probability and Informatics of Peoples' Friendship University of Russia (RUDN University), Moscow, Russian Federation

Yulia V. Gaidamaka, Doctor of Sciences in Physics and Mathematics, Professor, Professor of the Department of Applied Probability and Informatics of Peoples' Friendship University of Russia (RUDN University), Moscow, Russian Federation

Gleb Beliakov, PhD, Professor of Mathematics at Deakin University, Melbourne, Australia

Michal Hnatič, DrSc., Professor of Pavol Jozef Safarik University in Košice, Košice, Slovakia

Datta Gupta Subhashish, PhD in Physics and Mathematics, Professor of Hyderabad University, Hyderabad, India

Martikainen, Olli Erkki, PhD in Engineering, member of the Research Institute of the Finnish Economy, Helsinki, Finland

Mikhail V. Medvedev, Doctor of Sciences in Physics and Mathematics, Professor of the Kansas University, Lawrence, USA

Raphael Orlando Ramírez Inostroza, PhD professor of Rovira i Virgili University (Universitat Rovira i Virgili), Tarragona, Spain

Bijan Saha, Doctor of Sciences in Physics and Mathematics, Leading researcher in Laboratory of Information Technologies of the Joint Institute for Nuclear Research, Dubna, Russian Federation

Ochbadrah Chuluunbaatar, Doctor of Sciences in Physics and Mathematics, Leading researcher in the Institute of Mathematics, State University of Mongolia, Ulaanbaatar, Mongolia

Computer Design: *Anna V. Korolkova, Dmitry S. Kulyabov*

English text editors: *Nikolay E. Nikolaev, Ivan S. Zaryadov, Konstantin P. Lovetskiy*

Address of editorial board:

Ordzhonikidze St., 3, Moscow, Russia, 115419

Tel. +7 (495) 955-07-16, e-mail: publishing@rudn.ru

Editorial office:

Tel. +7 (495) 952-02-50, miphj@rudn.ru, dcm@sci.pfu.edu.ru

site: <http://journals.rudn.ru/miph>

Paper size 70×100/16. Offset paper. Offset printing. Typeface "Computer Modern".
Conventional printed sheet 6.29. Printing run 500 copies. Open price. The order 1220.

PEOPLES' FRIENDSHIP UNIVERSITY OF RUSSIA

6 Miklukho-Maklaya St., 117198 Moscow, Russia

Printed at RUDN Publishing House:

3 Ordzhonikidze St., 115419 Moscow, Russia,

Ph. +7 (495) 952-04-41; e-mail: publishing@rudn.ru



Contents

Anna V. Korolkova , Constitutive tensor in the geometrized Maxwell theory	305
Anna V. Korolkova, Migran N. Gevorkyan, Dmitry S. Kulyabov , Implementation of hyperbolic complex numbers in Julia language . . .	318
Oleg K. Kroytor, Mikhail D. Malykh , On a dispersion curve of a waveguide filled with inhomogeneous substance	330
Evgeniy B. Laneev, Obaida Baaj , On a modification of the Hamming method for summing discrete Fourier series and its application to solve the problem of correction of thermographic images	342
Konstantin P. Lovetskiy, Anton L. Sevastianov, Alexander V. Zorin , Profile thickness synthesis of thin-film waveguide Luneburg lens	357
Yu Ying, Zhen Lu , Conservative finite difference schemes for dynamical systems	364
Nikita A. Marusov , Approximation of radial structure of unstable ion-sound modes in rotating magnetized plasma column by eikonal equation	374



UDC 537.8:512.723

DOI: 10.22363/2658-4670-2022-30-4-305-317

Constitutive tensor in the geometrized Maxwell theory

Anna V. Korolkova

*Peoples' Friendship University of Russia (RUDN University),
6, Miklukho-Maklaya St., Moscow, 117198, Russian Federation*

(received: November 14, 2022; revised: December 12, 2022; accepted: December 19, 2022)

Abstract. It is generally accepted that the main obstacle to the application of Riemannian geometrization of Maxwell's equations is an insufficient number of parameters defining a geometrized medium. In the classical description of the equations of electrodynamics in the medium, a constitutive tensor with 20 components is used. With Riemannian geometrization, the constitutive tensor is constructed from a Riemannian metric tensor having 10 components. It is assumed that this discrepancy prevents the application of Riemannian geometrization of Maxwell's equations. It is necessary to study the scope of applicability of the Riemannian geometrization of Maxwell's equations. To determine whether the lack of components is really critical for the application of Riemannian geometrization. To determine the applicability of Riemannian geometrization, the most common variants of electromagnetic media are considered. The structure of the dielectric and magnetic permittivity is written out for them, the number of significant components for these tensors is determined. Practically all the considered types of electromagnetic media require less than ten parameters to describe the constitutive tensor. In the Riemannian geometrization of Maxwell's equations, the requirement of a single impedance of the medium is critical. It is possible to circumvent this limitation by moving from the complete Maxwell's equations to the approximation of geometric optics. The Riemannian geometrization of Maxwell's equations is applicable to a wide variety of media types, but only for approximating geometric optics.

Key words and phrases: geometrization of Maxwell's equations, permeability tensor, dielectric constant, magnetic permeability, geometric optics

1. Introduction

With the advent of the model Cayley–Klein [1, 2] the formalism of non-Euclidean spaces became used to describe physical models. This approach received popularity after the creation Einstein's general theory of relativity [3]. At the same time, there were attempts to geometrize Maxwell's electrodynamics [4–6].

However, this approach remained quite marginal until the golden age of theory of relativity [7, 8].

© Korolkova A. V., 2022



This work is licensed under a Creative Commons Attribution 4.0 International License

<https://creativecommons.org/licenses/by-nc/4.0/legalcode>

This direction became popular again in the new century and gave rise to the development of transformational optics [9–12]. However, it became visible that Riemannian geometry is insufficient for geometrization of Maxwell's equations [13, 14].

In this paper, the author expects to figure out what could hinder the application of Riemannian geometrization of Maxwell's equations and what is the scope of its applicability. To do this, we consider different electromagnetic media options and the limitations imposed by them are studied for possible geometrizations.

1.1. Article structure

In paragraph 1.2 we provide basic notation and conventions used in the article. In the section 1.3 we consider the limitation only for the case of a local linear medium. In the section 2 the constitutive tensor is formulated in a six-dimensional space. This is being done for clarity, to represent it as a matrix 6×6 . In the section 3 the reader is reminded of Riemannian geometrization of Maxwell's equations.

1.2. Notations and conventions

1. Greek indexes (α, β) will relate to a four-dimensional space and in a component form will have the following values: $\alpha = \overline{0, 3}$.
2. Latin indexes from the middle of the alphabet (i, j, k) will refer to three-dimensional space and in component form will have the following values: $i = \overline{1, 3}$.
3. In uppercase Latin letters denote the indices of the six-dimensional spaces: $I = \overline{1, 6}$.
4. To write the equations of electrodynamics in the work is used symmetrical CGS system [15].

1.3. The variations of physical environment

It is possible to consider several options for setting the constitutive laws depending on the medium (see Table 1).

Table 1

Constitutive laws depending on the medium

Medium type	Local case	Non-local case
Linear medium	$G^{\alpha\beta} = \lambda^{\alpha\beta\gamma\delta} F_{\gamma\delta}$	$G(x) = \int \lambda(x, s) \wedge F(s) ds$
Non-linear medium	$G^{\alpha\beta} = \lambda(F_{\gamma\delta})$	$G(x) = \int \lambda(x, F(s)) ds$

Tensors $F_{\alpha\beta}$ and $G^{\alpha\beta}$ have a sense of curvature in cotangent (T^*X) and tangent (TX) bundles.

In the linear local case, the tensors $F_{\alpha\beta}$ and $G^{\alpha\beta}$ are connected using fourth rang tensors.

In the linear non-local case, the connection is carried out using an integral kernel. However, in the presence of translational symmetry, the linear nonlocal case is reduced to the linear local case using the Fourier transform [16]. The non-local linear relationship between F and G looks in this case as follows:

$$G(x) = \int \lambda(x, s) \wedge F(s) ds. \tag{1}$$

In the case of translational invariance $\lambda(x, s) = \lambda(x - s)$ the relationship between F and G will have the form:

$$G^{\alpha\beta}(\omega, k_i) = \lambda^{\alpha\beta\gamma\delta}(\omega, k_i) F_{\gamma\delta}(\omega, k_i). \tag{2}$$

In the case of a nonlinear medium, it is assumed that through the linearization procedure, a tensor term similar to the local linear case can be distinguished in it.

Thus, it seems sufficient to consider only the local linear case.

2. Structure of the constitutive tensor

2.1. Representation of the constitutive tensor in space \mathbb{R}^4

The constitutive tensor $\lambda_{\gamma\delta}^{\alpha\beta}$ is a 4-tensor. We assume that the mapping $\lambda : \Lambda^2 M \rightarrow \Lambda_2 M$ is linear and local. Then it can be represented in the following form:

$$G^{\alpha\beta} = \lambda^{\alpha\beta\gamma\delta} F_{\gamma\delta}. \tag{3}$$

Here $\lambda^{\alpha\beta\gamma\delta}$ is a constitutive tensor containing information about both permeability and permittivity and electromagnetic connection [4–6, 17]. It can be seen that $\lambda^{\alpha\beta\gamma\delta}$ has the following symmetry:

$$\lambda^{\alpha\beta\gamma\delta} = \lambda^{[\alpha\beta][\gamma\delta]}.$$

To clarify the symmetry, the tensor $\lambda^{\alpha\beta\gamma\delta}$ can be represented as follows:

$$\lambda^{\alpha\beta\gamma\delta} = {}^{(1)}\lambda^{\alpha\beta\gamma\delta} + {}^{(2)}\lambda^{\alpha\beta\gamma\delta} + {}^{(3)}\lambda^{\alpha\beta\gamma\delta}.$$

The components of the tensor have the following symmetry:

$${}^{(1)}\lambda^{\alpha\beta\gamma\delta} = \lambda^{([\alpha\beta][\gamma\delta])}, \quad {}^{(2)}\lambda^{\alpha\beta\gamma\delta} = \lambda^{[[\alpha\beta][\gamma\delta]]}, \quad {}^{(3)}\lambda^{\alpha\beta\gamma\delta} = \lambda^{[\alpha\beta\gamma\delta]}.$$

Obviously, in this case $\lambda^{\alpha\beta\gamma\delta}$ has 36 independent components, ${}^{(1)}\lambda^{\alpha\beta\gamma\delta}$ has 20 independent components (*principal part*), ${}^{(2)}\lambda^{\alpha\beta\gamma\delta}$ has 15 independent components (*skewon*), ${}^{(3)}\lambda^{\alpha\beta\gamma\delta}$ has one independent component (*axion*).

We will consider only part of $(1)\lambda^{\alpha\beta\gamma\delta}$. For this case, we write down the material equations:

$$\begin{cases} D^i = \varepsilon^{ij} E_j + (1)\gamma_j^i B^j, \\ H_i = (\mu^{-1})_{ij} B^j + (2)\gamma_i^j E_j, \end{cases} \quad (4)$$

where ε^{ij} and μ^{ij} are the tensors of dielectric and magnetic permeability, $(1)\gamma_j^i$ and $(2)\gamma_j^i$ are cross terms.

Taking into account the structure of the tensors $F_{\alpha\beta}$ and $G^{\alpha\beta}$, as well as the constraints equations, we write:

$$\begin{aligned} F_{0i} &= E_i, & G^{0i} &= -D^i, \\ G^{ij} &= -e^{ijk} H_k, & F_{ij} &= -e_{ijk} B^k. \end{aligned} \quad (5)$$

Here the alternating tensor is denoted by e_{ijk} .

2.2. Representation of constitutive tensors in $A_2(\mathbb{R}^4)$ and $A^2(\mathbb{R}^{4*})$ spaces

Consider vector spaces $A^2(\mathbb{R}^{4*})$ and $A_2(\mathbb{R}^4)$ as typical layers of bundles $\Lambda^2 M$ and $\Lambda_2 M$ and we will make the transition to a six-dimensional space. Basis $A_2(\mathbb{R}^4)$ in this case has the form ζ_I , $I = 1, \dots, 6$, and the basis $A^2(\mathbb{R}^{4*})$ consists of components ζ^I , $I = 1, \dots, 6$. Let δ_μ , $\mu = 0, \dots, 3$ be the basis in \mathbb{R}^4 , and δ^μ , $\mu = 0, \dots, 3$ — the basis in \mathbb{R}^{4*} . Define the basis ζ_I in $A_2(\mathbb{R}^4)$ as follows:

$$\zeta_i = \delta_0 \wedge \delta_i, \quad \zeta_{i+3} = \frac{1}{2} \varepsilon_{ijk} \delta_j \wedge \delta_k, \quad i, j, k = 1, \dots, 3, \quad (6)$$

and basis ζ^I in $A^2(\mathbb{R}^{4*})$ in form

$$\zeta^i = \delta^0 \wedge \delta^i, \quad \zeta^{i+3} = \frac{1}{2} \varepsilon^{ijk} \delta^j \wedge \delta^k, \quad i, j, k = 1, \dots, 3. \quad (7)$$

Then the intensity of the electromagnetic field F can be represented as follows:

$$F = E_i \zeta^i + B_i \zeta^{i+3}. \quad (8)$$

We split the tensor λ^{IJ} such as

$$\lambda^{IJ} = (1)\lambda^{IJ} + (2)\lambda^{IJ} + (3)\lambda^{IJ}.$$

The components of the tensor λ^{IJ} have the following symmetry:

$$(1)\lambda^{IJ} = \lambda^{(IJ)} - \lambda_K^K \tilde{I}^{IJ}, \quad (2)\lambda^{IJ} = \lambda^{[IJ]}, \quad (3)\lambda^{IJ} = \lambda_K^K \tilde{I}^{IJ},$$

$$\tilde{I} := \begin{pmatrix} 0 & I^{ij} \\ I^{ij} & 0 \end{pmatrix}.$$

We indicate the number of components in these tensors:

- $(1)\lambda^{IJ}$ has 20 components;
- $(2)\lambda^{IJ}$ has 15 components;
- $(3)\lambda^{IJ}$ has 1 component.

Let's write out the main part of the constitutive tensor:

$${}^{(1)}\lambda^{IJ} = \begin{pmatrix} -\varepsilon^{ij} & {}^{(1)}\gamma_j^i \\ {}^{(2)}\gamma_i^j & \tilde{\mu}_{ij} \end{pmatrix}, \quad \tilde{\mu}_{ij} := (\mu^{-1})_{ij}. \tag{9}$$

Later in this article we will omit the left index of the main part of the constitutive tensor.

3. Riemannian geometrization of Maxwell's equations

We assume that the bundle has the structure of a Riemannian manifold. In this case, we can introduce a Riemannian metric on the manifold, which:

- is symmetric: $g_{\alpha\beta} := g_{(\alpha\beta)}$;
- is consistent with connection: $\nabla_\alpha g^{\alpha\beta} := 0$.

This statement is equivalent to the fact that we use connection Levi-Civitas.

We introduce an effective metric based on the bundle $g_{\alpha\beta}$. Then the metric is induced into layers and the Lagrangian of the electromagnetic field can be written in the form of the Yang-Mills Lagrangian:

$$L = -\frac{1}{16\pi c} G^{\alpha\beta} F_{\alpha\beta} - \frac{1}{c^2} A_\alpha j^\alpha \sqrt{-g},$$

which is equivalent to the following entry

$$L = -\frac{1}{16\pi c} g^{\alpha\gamma} g^{\beta\delta} F_{\alpha\beta} F_{\gamma\delta} \sqrt{-g} - \frac{1}{c^2} A_\alpha j^\alpha \sqrt{-g}.$$

Let's construct the tensor $\lambda^{\alpha\beta\gamma\delta}$ as follows:

$$\lambda^{\alpha\beta\gamma\delta} = \sqrt{-g} g^{\alpha\beta} g^{\gamma\delta} = \frac{\sqrt{-g}}{2} (g^{\alpha\gamma} g^{\beta\delta} + g^{\alpha\delta} g^{\beta\gamma}) + \frac{\sqrt{-g}}{2} (g^{\alpha\gamma} g^{\beta\delta} - g^{\alpha\delta} g^{\beta\gamma}).$$

Then the material equations will take the following form (for symmetry reasons):

$$G^{\alpha\beta} = \frac{\sqrt{-g}}{2} (g^{\alpha\gamma} g^{\beta\delta} - g^{\alpha\delta} g^{\beta\gamma}) F_{\gamma\delta}.$$

In the case of writing by components, we get the following expressions:

$$\begin{aligned} G^{0i} &= \frac{\sqrt{-g}}{2} (g^{00} g^{ij} - g^{0i} g^{0j}) F_{0j} + \frac{\sqrt{-g}}{2} (g^{0j} g^{ik} - g^{0k} g^{ij}) F_{jk}, \\ G^{ij} &= \frac{\sqrt{-g}}{2} (g^{i0} g^{jk} - g^{0j} g^{ik}) F_{0k} + \frac{\sqrt{-g}}{2} (g^{ik} g^{jl} - g^{il} g^{jk}) F_{kl}. \end{aligned} \tag{10}$$

Formally, it is possible to write out an expression for the permittivity:

$$\varepsilon^{ij} = -\sqrt{-g}(g^{00}g^{ij}-g^{0i}g^{0j}) \quad (11)$$

and the expression for magnetic permeability:

$$(\mu^{-1})_{ij} = \sqrt{-g}\varepsilon_{mni}\varepsilon_{klj}g^{nk}g^{ml}. \quad (12)$$

Thus the geometrized connection equations in coordinates have the following form:

$$\begin{aligned} D^i &= \varepsilon^{ij}E_j + {}^{(1)}\gamma_j^i B^j, \\ H_i &= (\mu^{-1})_{ij}B^j + {}^{(2)}\gamma_i^j E_j, \\ \varepsilon^{ij} &= -\sqrt{-g}(g^{00}g^{ij}-g^{0i}g^{0j}), \\ (\mu^{-1})_{ij} &= \sqrt{-g}\varepsilon_{mni}\varepsilon_{klj}g^{nk}g^{ml}, \\ {}^{(1)}\gamma_j^i &= {}^{(2)}\gamma_j^i = \sqrt{-g}\varepsilon_{klj}g^{0k}g^{il}. \end{aligned} \quad (13)$$

Statement. Let the space be represented as $\mathbb{R}^4 = \mathbb{R}^1 \times \mathbb{R}^3$. Then in Riemannian geometrization, under the condition $g^{0i} = 0$, the equality holds

$$\varepsilon^{ij} = \mu^{ij}. \quad (14)$$

Proof. Note that $\Delta_{ij} = \varepsilon_{mni}\varepsilon_{klj}g^{nk}g^{ml}$ is an algebraic complement for g^{ij} . Then

$$\varepsilon^{ij}(\mu^{-1})_{ip} = -\sqrt{-g}g^{00}g^{ij}\sqrt{-g}\varepsilon_{mni}\varepsilon_{klp}g^{nk}g^{ml} = gg^{00}\det\{g^{kl}\}\delta_p^j = \delta_p^j.$$

It follows that $\varepsilon^{ij} = \mu^{ij}$. □

Then the geometrized constitutive tensor has the following form:

$$\lambda^{IJ} = \begin{pmatrix} -\varepsilon^{ij} & {}^{(1)}\gamma_j^i \\ {}^{(2)}\gamma_i^j & (\varepsilon^{-1})_{ij} \end{pmatrix}. \quad (15)$$

Consider the limitations of this approach:

1. Since the metric tensor g_{ij} has 10 components, the geometrized constitutive tensor cannot have more than 10 independent components.
2. Given the constitutive equations, only media with a single impedance can be considered.

However, the geometrized version can be used to approximate geometric optics when the dielectric ε^{ij} and magnetic μ_{ij} permeability are not used separately. Instead, in the approximation of geometric optics, the refractive index of the medium is used:

$$n_j^i = \sqrt{\varepsilon_k^i \mu_j^k}. \quad (16)$$

In this case, the geometrized constitutive tensor has the following form:

$$\lambda^{IJ} = \begin{pmatrix} -(\sqrt{n})^{ij} & ({}^{(1)}\gamma_j^i) \\ ({}^{(2)}\gamma_i^j) & (\frac{1}{\sqrt{n}})_{ij} \end{pmatrix}. \quad (17)$$

4. Examples of media

4.1. Linear isotropic media

The most elementary electromagnetic media are linear isotropic media, such as classical vacuum. The term *isotropic* refers to invariance with respect to spatial rotations in the selected frame of reference. The rotation of any closed system as a whole does not change its physical properties. There is no particular direction in space with respect to which there is any special symmetry. All directions are equal. The electromagnetic properties of the medium do not depend on the direction. In this case, the elements of the tensor λ^{IJ} are represented as:

$$\varepsilon^{ij} = \varepsilon(x^i)\delta^{ij}, \quad \tilde{\mu}_{ij} := (\mu^{-1}(x^i))\delta_{ij}, \quad ({}^{(1)}\gamma_j^i = 0, \quad ({}^{(2)}\gamma_i^j = 0$$

or in matrix form:

$$\lambda^{IJ} = \begin{pmatrix} -\varepsilon(x^i)\delta^{ij} & 0 \\ 0 & \mu^{-1}(x^i)\delta_{ij} \end{pmatrix}. \quad (18)$$

In this case, the permeability matrix contains only two independent components in the laboratory reference frame. Function $\varepsilon(x^i)$ is called the dielectric constant of the medium. Function $\mu(x^i)$ is called the magnetic permeability of the medium. When these functions are constant in the selected frame of reference, the medium is called *homogeneous*.

The classical electromagnetic vacuum is assumed to be linear, isotropic and homogeneous. Its dielectric constant (in the SI system) is denoted by ε_0 , and the magnetic permeability is denoted by μ_0 .

The application of a geometrized constitutive tensor is possible in the approximation of geometric optics. In this case λ^{IJ} will have the form:

$$\lambda^{IJ} = \begin{pmatrix} -\sqrt{n(x^i)}\delta^{ij} & 0 \\ 0 & \frac{1}{\sqrt{n(x^i)}}\delta_{ij} \end{pmatrix}. \quad (19)$$

In this case, the permeability matrix contains only one independent component.

4.2. Linear optical medium

It is assumed that the permittivity ε^{ij} can be inhomogeneous and (or) anisotropic. Heterogeneity is most common when matrix components are

piecewise constant and undergo discontinuities at the interface of heterogeneous media. Since the magnetic permeability of optical media is neglected, they are considered to be dielectric media:

$$(\mu^{-1})_{ij} = \delta_{ij}. \quad (20)$$

If the permittivity ε^{ij} is anisotropic, but at the same time symmetrical, then it is possible to determine the main reference point in which it takes the form of a diagonal matrix:

$$\varepsilon^{ij} := \text{diag}(\varepsilon_x, \varepsilon_y, \varepsilon_z). \quad (21)$$

The diagonal elements represented by the main permittivity are in this case the eigenvalues of the matrix

$$\varepsilon_j^i = \varepsilon^{ik} g_{jk}. \quad (22)$$

Since the matrix ε^{ij} is symmetric, then the eigenvalues exist and are valid, and the eigenvectors are orthogonal.

Media variants:

- when all eigenvalues are equal, the medium is called isotropic;
- when two eigenvalues are equal, and the third is different from them, the medium is called uniaxial anisotropic;
- when all three eigenvalues are unequal, the medium is called biaxial anisotropic.

More generally, the magnetic permeability is not singular:

$$(\mu^{-1})_{ij} = \text{diag}((\mu^{-1})_x, (\mu^{-1})_y, (\mu^{-1})_z), \quad (23)$$

and λ^{IJ} can be represented as a matrix:

$$\lambda^{IJ} = \text{diag}(-\varepsilon_x(x^i), -\varepsilon_y(x^i), -\varepsilon_z(x^i), \mu_x^{-1}(x^i), \mu_y^{-1}(x^i), \mu_z^{-1}(x^i)). \quad (24)$$

The application of a geometrized constitutive tensor is possible in the approximation of geometric optics. Then the tensor λ^{IJ} will take the form:

$$\lambda^{IJ} = \text{diag} \left(-\sqrt{n_x(x^i)}, -\sqrt{n_y(x^i)}, -\sqrt{n_z(x^i)}, \frac{1}{\sqrt{n_x(x^i)}}, \frac{1}{\sqrt{n_y(x^i)}}, \frac{1}{\sqrt{n_z(x^i)}} \right).$$

In this case, the permeability matrix contains three independent components.

4.3. Bi-isotropic media

The special properties of these media are due to the connection between electric and magnetic fields, which can be described by some defining relations. Bi-isotropic media can change the polarization of light either by refraction or by transmission [18]. These media are similar to isotropic media, but the cross terms are not zero.

The coupling equations in the case of an isotropic medium have the following form:

$$\begin{aligned} D^i &= \varepsilon g^{ij} E_j + \gamma g_j^i B^j, \\ H_i &= (\mu^{-1}) g_{ij} B^j + \gamma g_i^j E_j. \end{aligned} \tag{25}$$

The elements of the tensor λ^{IJ} have the form:

$$\varepsilon^{ij} = \varepsilon(x^i) g^{ij}, \quad (\mu^{-1})_{ij} := (\mu^{-1}(x^i)) g_{ij}, \quad (1)\gamma_j^i = \gamma(x^i) g_j^i, \quad (2)\gamma_i^j = \gamma(x^i) g_i^j.$$

In matrix form, the tensor λ^{IJ} for a bi-isotropic medium will have the form:

$$\lambda^{IJ} = \begin{pmatrix} -\varepsilon(x^i) g^{ij} & \gamma(x^i) g_j^i \\ \gamma(x^i) g_i^j & \mu^{-1}(x^i) g_{ij} \end{pmatrix}. \tag{26}$$

For the case of geometric optics, the tensor λ^{IJ} for a bi-isotropic medium will take the form:

$$\lambda^{IJ} = \begin{pmatrix} -\sqrt{n(x^i)} g^{ij} & \gamma(x^i) g_j^i \\ \gamma(x^i) g_i^j & n^{-1/2}(x^i) g_{ij} \end{pmatrix}. \tag{27}$$

The permeability matrix in this case contains two independent components.

4.4. Bi-anisotropic media

In bi-anisotropic media, the dielectric constant, magnetic permeability, and coupling coefficient are complete tensors. In this case, the coupling equations have the following form:

$$\begin{aligned} D^i &= \varepsilon^{ij} E_j + (1)\gamma_j^i B^j, \\ H_i &= (\mu^{-1})_{ij} B^j + (2)\gamma_i^j E_j. \end{aligned} \tag{28}$$

The elements of the tensor λ^{IJ} take the form

$$\varepsilon^{ij} := \varepsilon^{ij}(x^i), \quad (\mu^{-1})_{ij} := (\mu^{-1}(x^i))_{ij}, \quad (1)\gamma_j^i = \gamma_j^i(x^i), \quad (2)\gamma_i^j = \gamma_i^j(x^i).$$

In matrix form, the tensor λ^{IJ} for a bi-isotropic medium has the form:

$$\lambda^{IJ} = \begin{pmatrix} -\varepsilon^{ij}(x^i) & \gamma_j^i(x^i) \\ \gamma_i^j(x^i) & (\mu^{-1})_{ij}(x^i) \end{pmatrix}. \tag{29}$$

For the case of geometric optics, the tensor λ^{IJ} for a bi-anisotropic medium is represented as:

$$\lambda^{IJ} = \begin{pmatrix} -(\sqrt{n})^{ij}(x^i) & \gamma_j^i(x^i) \\ \gamma_i^j(x^i) & (n^{-1/2})_{ij}(x^i) \end{pmatrix}. \tag{30}$$

In this case, the permeability matrix contains twenty independent components.

Thus, the following conclusions can be drawn:

- in most practical cases, it is necessary to take into account less than ten components of the tensor λ^{IJ} ;
- for the case of an anisotropic medium, more than ten components of the constitutive tensor should be taken into account.

5. Conclusion

When applying the Riemannian geometrization of Maxwell's equations, two significant obstacles arise.

It is usually considered that the main obstacle to the application of Riemannian geometrization of Maxwell's equations is an insufficient number of parameters defining a geometrized medium. It is known that in the classical description of the equations of electrodynamics in the medium, a constitutive tensor with 20 components is used, and in Riemannian geometrization, the constitutive tensor is constructed from a Riemannian metric tensor with only 10 components. Thus, most authors point out that the main limitation of the application of Maxwell's geometrized theory is the number of free components in the constitutive tensor. However, this is not the case. It is enough to consider the most popular variants of electromagnetic media to make sure that in practically used cases the number of components is significantly less than ten.

Another limitation is that Maxwell's geometrized theory in the case of Riemannian geometrization requires that the medium has a unit impedance. This restriction is too strong in the general case. It seems that the geometrized Maxwell theory in the case of Riemannian geometrization is not applicable in the case of the complete Maxwell theory and in the case of the approximation of the wave equation. But this limitation can be circumvented by switching to the approximation of geometric optics, since in this case the impedance of the medium is not taken into account.

Thus, we can conclude that Maxwell's geometrized theory in the case of Riemannian geometrization is applicable to the description of Maxwell's theory, but mainly for the case of approximation of geometric optics.

Acknowledgments

This paper has been supported by the RUDN University Strategic Academic Leadership Program.

References

- [1] F. C. Klein, "Ueber die sogenannte Nicht-Euklidische Geometrie," German, in *Gauß und die Anfänge der nicht-euklidischen Geometrie*, ser. Teubner-Archiv zur Mathematik, vol. 4, Wien: Springer-Verlag Wien, 1985, pp. 224–238. DOI: 10.1007/978-3-7091-9511-6_5.

- [2] F. C. Klein, "A comparative review of recent researches in geometry," *Bulletin of the American Mathematical Society*, vol. 2, no. 10, pp. 215–249, 1893. DOI: 10.1090/S0002-9904-1893-00147-X.
- [3] C. W. Misner, K. S. Thorne, and J. A. Wheeler, *Gravitation*. San Francisco: W. H. Freeman, 1973.
- [4] I. Y. Tamm, "Crystal optics theory of relativity in connection with geometry biquadratic forms," vol. 57, no. 3-4, pp. 209–240, 1925, in Russian.
- [5] I. Y. Tamm, "Electrodynamics of an anisotropic medium in a special theory of relativity," *Russian Journal of Physical and Chemical Society. Part physical*, vol. 56, no. 2-3, pp. 248–262, 1924, in Russian.
- [6] L. I. Mandelstam and I. Y. Tamm, "Elektrodynamik der anisotropen Medien in der speziellen Relativitätstheorie," German, *Mathematische Annalen*, vol. 95, no. 1, pp. 154–160, 1925.
- [7] J. Plebanski, "Electromagnetic waves in gravitational fields," *Physical Review*, vol. 118, no. 5, pp. 1396–1408, 1960. DOI: 10.1103/PhysRev.118.1396.
- [8] F. Felice, "On the gravitational field acting as an optical medium," *General Relativity and Gravitation*, vol. 2, no. 4, pp. 347–357, 1971. DOI: 10.1007/BF00758153.
- [9] A. J. Ward and J. B. Pendry, "Refraction and geometry in Maxwell's equations," *Journal of Modern Optics*, vol. 43, no. 4, pp. 773–793, Apr. 1996. DOI: 10.1080/09500349608232782.
- [10] U. Leonhardt and T. G. Philbin, "Transformation optics and the geometry of light," in *Progress in Optics*. 2009, vol. 53, ch. 2. DOI: 10.1016/S0079-6638(08)00202-3.
- [11] U. Leonhardt and T. G. Philbin, "General Relativity in Electrical Engineering," vol. 8, 247, pp. 247.1–18, 2006. DOI: 10.1088/1367-2630/8/10/247.
- [12] D. S. Kulyabov, A. V. Korolkova, L. A. Sevastianov, M. N. Gevorkyan, and A. V. Demidova, "Geometrization of Maxwell's Equations in the Construction of Optical Devices," in *Proceedings of SPIE. Saratov Fall Meeting 2016: Laser Physics and Photonics XVII and Computational Biophysics and Analysis of Biomedical Data III*, vol. 10337, SPIE, 2017. DOI: 10.1117/12.2267959.
- [13] D. S. Kulyabov, A. V. Korolkova, and T. R. Velieva, "The Riemannian Geometry is not Sufficient for the Geometrization of the Maxwell's Equations," in *Proceedings of SPIE. Saratov Fall Meeting 2017: Laser Physics and Photonics XVIII; and Computational Biophysics and Analysis of Biomedical Data IV*, vol. 10717, Saratov: SPIE, Apr. 2018. DOI: 10.1117/12.2315204.
- [14] D. S. Kulyabov, A. V. Korolkova, T. R. Velieva, and A. V. Demidova, "Finslerian representation of the Maxwell equations," in *Proceedings of SPIE. Saratov Fall Meeting 2018: Laser Physics, Photonic Technologies, and Molecular Modeling*, vol. 11066, Saratov: SPIE, Jun. 2019. DOI: 10.1117/12.2525534.

- [15] D. V. Sivukhin, “The international system of physical units,” *Soviet Physics Uspekhi*, vol. 22, no. 10, pp. 834–836, Oct. 1979. DOI: 10.1070/pu1979v022n10abeh005711.
- [16] D. S. Kulyabov, A. V. Korolkova, and V. I. Korolkov, “Maxwell’s equations in arbitrary coordinate system,” *Bulletin of Peoples’ Friendship University of Russia. Series “Mathematics. Information Sciences. Physics”*, no. 1, pp. 96–106, 2012.
- [17] L. D. Landau, E. M. Lifshitz, and L. P. Pitaevskii, *Course of Theoretical Physics*, 2nd. Butterworth-Heinemann, 1984, vol. 8, 460 pp.
- [18] S. Bolioli, “Bi-Isotropic and Bi-Anisotropic Media,” in *Advances in Complex Electromagnetic Materials. NATO ASI Series*. Springer Netherlands, 1997, vol. 28, ch. 3, pp. 33–51. DOI: 10.1007/978-94-011-5734-6_3.

For citation:

A. V. Korolkova, Constitutive tensor in the geometrized Maxwell theory, *Discrete and Continuous Models and Applied Computational Science* 30 (4) (2022) 305–317. DOI: 10.22363/2658-4670-2022-30-4-305-317.

Information about the authors:

Korolkova, Anna V. — Docent, Candidate of Sciences in Physics and Mathematics, Associate Professor of Department of Applied Probability and Informatics of Peoples’ Friendship University of Russia (RUDN University) (e-mail: korolkova-av@rudn.ru, phone: +7(495) 952-02-50, ORCID: <https://orcid.org/0000-0001-7141-7610>)

УДК 537.8:512.723

DOI: 10.22363/2658-4670-2022-30-4-305-317

Тензор проницаемостей в геометризованной теории Максвелла

А. В. Королькова

*Российский университет дружбы народов,
ул. Миклухо-Маклая, д. 6, Москва, 117198, Россия*

Аннотация. Считается, что основным препятствием к применению римановой геометризации уравнений Максвелла является недостаточное количество параметров, задающих геометризованную среду. При классическом описании уравнений электродинамики в среде используется тензор проницаемостей, имеющий 20 компонент. При римановой геометризации тензор проницаемостей строится из риманового метрического тензора, имеющего только 10 компонент. Предполагается, что данное несоответствие мешает применению римановой геометризации уравнений Максвелла. В статье предложено определить, действительно ли недостаток компонент является критическим для применения римановой геометризации уравнений Максвелла. Для определения области применимости римановой геометризации рассмотрены наиболее распространённые варианты электромагнитных сред. Для них выписана структура диэлектрической и магнитной проницаемостей, определено количество значащих компонент для этих тензоров. Показано, что практически все рассмотренные типы электромагнитных сред требуют менее десяти параметров для описания тензора проницаемостей. При римановой геометризации уравнений Максвелла критическим является требование единичного импеданса среды. Обойти данное ограничение возможно путём перехода от полных уравнений Максвелла к приближению геометрической оптики. Показано, что риманова геометризация уравнений Максвелла применима для большого разнообразия типов среды, но только для приближения геометрической оптики.

Ключевые слова: геометризация уравнений Максвелла, тензор проницаемостей, диэлектрическая проницаемость, магнитная проницаемость, геометрическая оптика



UDC 511.14:004.432

DOI: 10.22363/2658-4670-2022-30-4-318-329

Implementation of hyperbolic complex numbers in Julia language

Anna V. Korolkova¹,
Migran N. Gevorkyan¹, Dmitry S. Kulyabov^{1,2}

¹ Peoples' Friendship University of Russia (RUDN University),
6, Miklukho-Maklaya St., Moscow, 117198, Russian Federation

² Joint Institute for Nuclear Research,
6, Joliot-Curie St., Dubna, Moscow Region, 141980, Russian Federation

(received: November 7, 2022; revised: December 12, 2022; accepted: December 19, 2022)

Abstract. Hyperbolic complex numbers are used in the description of hyperbolic spaces. One of the well-known examples of such spaces is the Minkowski space, which plays a leading role in the problems of the special theory of relativity and electrodynamics. However, such numbers are not very common in different programming languages. Of interest is the implementation of hyperbolic complex in scientific programming languages, in particular, in the Julia language. The Julia language is based on the concept of multiple dispatch. This concept is an extension of the concept of polymorphism for object-oriented programming languages. To implement hyperbolic complex numbers, the multiple dispatching approach of the Julia language was used. The result is a library that implements hyperbolic numbers. Based on the results of the study, we can conclude that the concept of multiple dispatching in scientific programming languages is convenient and natural.

Key words and phrases: Julia programming language, multiple dispatch, abstract data types, type conversion, parametric structures, hyperbolic complex numbers

1. Introduction

The Julia programming language [1, 2] is a promising language for scientific computing. At the moment, the Julia language has reached a stable state. By design, Julia solves the *problem of two languages*. This problem lies in the fact that for rapid prototyping, data processing and visualization, an interpreted dynamic language or a mathematical package (Python, Matlab, etc.) is used, and for intensive numerical calculations, the program has to be rewritten in a compiled language with static typing (C/ C++, Fortran).

An illustration of this problem can be seen in Python, which has gained wide popularity as an interface *language-gluе*. Numerous wrapper libraries were written on it, which used Python code to call C/C++ and Fortran functions from precompiled libraries. For example, the well-known library



NumPy [3] consists of 51% C code and only 47% Python code (the remaining percentages are divided between C++, Fortran, JavaScript and Unix shell).

The Julia language combines the flexibility of dynamically typed interpreted languages with the performance of statically typed compiled languages.

The basic part of the Julia language is very similar to other scientific programming languages, so it does not cause difficulties in mastering. However, Julia's core is built around the concept of *multiple dispatch* [4], which is rare in other languages. It is in this mechanism that the essential difference of Julia from other languages lies, and its understanding is essential for the full use of all the advantages of Julia.

In the article, the authors paid great attention to illustrating the mechanism of multiple dispatch and other mechanisms that are closely related to it.

In the first part of the article, we give the necessary definitions and illustrate the concept of multiple dispatch with simple examples that allow you to understand the syntax associated with this part of the language and capture the essence of this approach. In the second part, we give an example of the implementation of hyperbolic complex numbers in the Julia language. This example allows you to touch not only multiple dispatch, but also the type casting mechanism, the abstract type hierarchy, overloading arithmetic operators, and specifying user-defined data types.

2. Multiple dispatch

2.1. Common definitions

Dynamic dispatch is a mechanism that allows you to choose which of the many implementations of a polymorphic function (or operator) should be called in a given case [5]. In this case, the choice of one or another implementation is carried out at the stage of program execution. *Multiple dispatch* is based on dynamic dispatch. In this case, the choice of implementation of a polymorphic function is made based on the type, number, and order of the function's arguments. This is how runtime polymorphic dispatch is implemented [6, 7]. Note also that in addition to the term multiple dispatch, the term *multimethod* is also used.

The mechanism of multiple dispatch is similar to the mechanism of overloading functions and operators, implemented, for example, in the C++ language. Function overloading, however, is done exclusively at compile time, while multiple dispatch should work at runtime as well (runtime polymorphism).

2.2. Multiple dispatch in Julia

To illustrate the mechanism of multiple dispatch, we will give the following code example in the Julia language:

```
function f(x, y)
    println("Generic implementation")
    return x + y
end
```

```
function f(x)
    println("For single argument")
```

```
    return x
end

function f(x::Integer, y::Integer)
    println("Implementation for integers")
    return x + y
end

function f(x::String, y::String)
    println("Implementation for strings")
    return x * " " * y
end

function f(x::Tuple{Int, Int}, y::Tuple{Int, Int})
    println("Implementation for tuples of two integer elements")
    return (x[1], x[2], y[1], y[2])
end
```

In this example, we have created five implementations of the f function, which differ from each other in different signatures. In terms of the Julia language, this means that one function f now has four different *methods*. In the first two methods, we did not use type annotations, so the type of the arguments will be determined either at compile time or at run time (as in interpreted languages). It is also worth noting that Julia uses dynamic JIT compilation (just-in-time), so the compilation stage is not explicitly separated from the execution stage for the user.

The arguments of the following three methods are annotated with types, so they will only be called if the types match the annotations. In the f for strings, the $*$ concatenation operator is used. The choice of the multiplication sign $*$ instead of the more traditional addition sign $+$ is justified by the creators of the language by the fact that string concatenation is not a commuting operation, so it is more logical to use the multiplication sign for it, rather than the addition sign, which is often used to denote commuting operations.

The following code snippet illustrates how multiple dispatch works at compile time. The `@show` macro is used to print out the name of the function and the arguments passed to it:

```
@show f(2.0, 1)
@show f(2, 2)
@show f(0x2, 0x1) # numbers in hexadecimal system
@show f("Text", "line")
@show f(3)
@show f([1, 2], [3, 4])
@show f((1, 2), (3, 4))
```

- In the first line, we passed real (floating-point) type arguments to the function, so a generic implementation call was made. Since the operator $+$ is defined for floating point numbers, the function succeeded and gave the correct result.
- Methods for integers were called in the second and third lines. Note that the `Integer` type is an *abstract* type and includes signed and unsigned integers from 1 to 16 bytes in size, defined in the language core. Numbers written in hexadecimal are interpreted by default as unsigned integers.

- The method for strings was called on the fourth line. In the fifth line, the method for one argument.
- The sixth line passed two arrays as arguments. The + operation is defined for arrays, so the function ran without error and returned an element-wise sum.
- In the seventh line, the function arguments are tuples consisting of two integers. Since we defined a method for such a combination of arguments, the function worked correctly.

The result of executing the code looks like:

```

Generic implementation
f(2.0, 1) = 3.0
Implementation for integers
f(2, 2) = 4
Implementation for integers
f(0x02, 0x01) = 0x03
Implementation for strings
f("Text", "line") = "Text line"
For single argument
f(3) = 3
Generic implementation
f([1, 2], [3, 4]) = [4, 6]
Implementation for tuples of two integer elements
f((1, 2), (3, 4)) = (1, 2, 3, 4)

```

The above example works correctly in languages that support function overloading and does not demonstrate the specifics of dynamic dispatching, since the types of arguments are known at the compilation stage and are available to the translator.

To test the work of dynamic method calls, consider the following code:

```

print("Enter an integer:")
# Read a string and convert to an integer type
@show n = parse{Int32, readline()}
if n > 0
    x = 1.2; y = 0.1
else
    x = 1; y = 2
end
f(x, y)

```

Here, the types of variable values x and y are not known at compile time, as they depend on what number the user enters during program execution. However, for the case of integer x and y the corresponding method is called.

3. Hyperbolic numbers

We will use hyperbolic numbers to illustrate the multiple dispatch capabilities of the Julia language, so we will limit ourselves to the definition and basic arithmetic operations.

Hyperbolic numbers [8–11], along with elliptic and parabolic numbers, are a generalization of complex numbers. Hyperbolic numbers can be defined as follows:

$$z = x + jy, \quad j^2 = 1, \quad j \neq \pm 1. \quad (1)$$

The quantity j will be called the *hyperbolic imaginary unit*, and the quantities x and y will be called the real and imaginary parts, respectively.

For two hyperbolic numbers $z_1 = x_1 + jy_1$ and $z_2 = x_2 + jy_2$ the following arithmetic operations are performed.

Addition $z_1 + z_2 = (x_1 + x_2) + j(y_1 + y_2)$.

Multiplication $z_1 z_2 = (x_1 x_2 + y_1 y_2) + j(x_1 y_2 + x_2 y_1)$.

Conjugation $z^* = x - jy$.

Inverse number $z^{-1} = \frac{x}{x^2 + y^2} - j \frac{y}{x^2 - y^2}$.

Division $\frac{z_1}{z_2} = \frac{x_1 x_2 - y_1 y_2}{x_2^2 - y_2^2} + j \frac{x_1 y_1 - x_2 y_2}{x_2^2 - y_2^2}$.

The implementation of hyperbolic numbers is in many respects similar to the implementation of complex ones. Operators $+$, $-$, $*$ must be overloaded, and $/$, root extraction, exponentiation, elementary math functions, etc. At the same time, for the purposes of illustrating the mechanism of operation of multiple dispatching, it is arithmetic operations that are of primary interest. This is due to the fact that elementary functions take only one argument, and it is enough to define only one method for them. In the case of arithmetic operators, it is necessary to provide combinations of arguments of different numeric types. So, for example, it should be possible to add a hyperbolic number to an integer, rational, irrational number, which automatically affects not only multiple dispatch, but also type casting mechanisms, an abstract type hierarchy, and default constructor overloading.

Therefore, we will confine ourselves to examples of the implementation of precisely arithmetic operations and that's all, without touching on the more mathematically complex calculations of various elementary functions of a hyperbolic number.

Note that in addition to the term hyperbolic numbers, there are also terms in the literature: double numbers, split complex numbers, perplex numbers, hyperbolic numbers [8, 12–15].

4. Implementation of hyperbolic numbers in Julia

4.1. Declaring a Data Structure

The implementation of hyperbolic numbers in Julia was based on the code for complex numbers available in the official Julia repository. We also used the developments obtained in the implementation of parabolic complex numbers [16]. New type `Hyperbolic` defined with an immutable structure:

```
struct Hyperbolic{T<:Real} <: Number
    "Real part"
    re::T
    "Imaginary part"
    jm::T
end
```

The structure is simple and contains only two fields of parametric type `T`. This requires that the type `T` was a subtype of the abstract type `Real` (syntax `T<:Real`). The type `Hyperbolic` is a subtype of the abstract type `Number`

(see figure 1). Thus, hyperbolic numbers are built into an already existing hierarchy of numeric types.

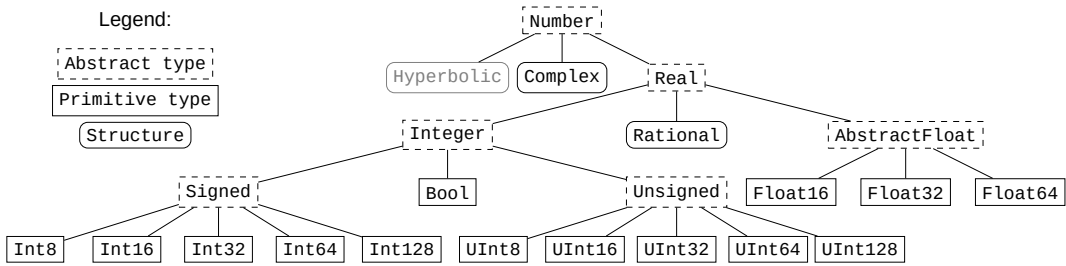


Figure 1. Location of hyperbolic numbers in Julia's type hierarchy

After the structure is defined, a new object of type `Hyperbolic` can be created by calling the default constructor. So, for example, the number $h = 1 + j3$ is given as follows:

```
h = Hyperbolic{Float64}(1, 3)
```

After creation, you can access the fields of the structure as `h.re` and `h.im`, but an attempt changing the value of a field of an already existing object will result in an error, since structures are immutable entities:

```
h = Hyperbolic(1, 3).
```

However, if the argument types are different, then the default constructor will not be able to implicitly cast and create a new object. In this case, you must explicitly specify the parametric type

```
# Float64 ≠ Int64
h = Hyperbolic(1.0, 3) # Error
h = Hyperbolic{Float64}(1.0, 3) # Correct
```

4.2. Additional constructors

The default constructor is a normal function whose name is the same as the type name. By creating additional methods for this function, you can create additional constructors to handle various special cases.

So, for example, in order not to specify a parametric type every time, you should add a new constructor of the following form:

```
"""Constructor #2"""
function Hyperbolic(x::Real, y::Real)
    return Hyperbolic(promote(x, y)...)
end
```

The `promote` function casts the arguments passed to it to a common type and returns the result as a tuple. Postfix operator `...` unpacks the tuple and passes its elements as arguments to the constructor function. The language core defines casting rules for all subtypes of the `Real` abstract type, so now the constructor will work correctly for any combination of arguments, as long as the `T<:Real` rule is fulfilled. For example, the following code will work correctly:

```
# Rational  $\pi$  Float64
h = Hyperbolic(1/3, pi)
>> Hyperbolic{Float64}(0.5, 3.141592653589793)
```

We passed a rational number (type **Rational**) and a built-in global constant (number π) of type **Float64** to the constructor. After that, the type casting rule worked and both arguments were cast to the type **Float64** as more general.

Declaring two more additional constructors will allow you to specify hyperbolic numbers with zero imaginary part:

```
"""Constructor №3"""
function Hyperbolic{T}(x::Real) where {T<:Real}
    return Hyperbolic{T}(x, 0)
end
"""Constructor №4"""
function Hyperbolic(x::Real)
    return Hyperbolic(promote(x, 0)...)
end
```

Constructor number 3 is a parametric function that is declared using the **where** construct. The **T** is a subtype of the abstract type **Real**. Constructor number 4 works similarly to constructor number 2.

Two more constructors will allow you to pass other hyperbolic numbers as an argument to the constructor:

```
"""Constructor №5"""
function Hyperbolic{T}(h::Hyperbolic) where {T<:Real}
    Hyperbolic{T}(h.re, h.jm)
end
"""Constructor №6"""
function Hyperbolic(h::Hyperbolic)
    return Hyperbolic(promote(h.re, h.jm)...)
end
```

For more convenience, you can also create a separate constant for the imaginary cost **j**:

```
const jm = Hyperbolic(0, 1)
```

4.3. Data printing

To be able to print hyperbolic type values in a compact and readable form, you should add the appropriate methods to the **show** function from the **Base** module:

```
function Base.show(io::IO, h::Hyperbolic)
    print(io, h.re, "+", h.jm, "j")
end
```

Function **show** is used when printing data to the console, in particular, it is called by the **println** and macro **@show**. The code and output listings below will assume that the **show** method has been added for hyperbolic numbers.

4.4. Type casting

Before proceeding to the implementation of methods for arithmetic operations with hyperbolic numbers, it is necessary to define the rules for type casting. To do this, create a new method for the function `promote_rule` from the `Base` module:

```
function Base.promote_rule(::Type{Hyperbolic{T}}, ::Type{S})
    ↪ where {T<:Real, S<:Real}
        return Hyperbolic{promote_type(T, S)}
    end
function Base.promote_rule(::Type{Hyperbolic{T}},
    ↪ ::Type{Hyperbolic{S}}) where {T<:Real, S<:Real}
        return Hyperbolic{promote_type(T, S)}
    end
```

As arguments in `promote_rule` parametric types are specified, which should be cast to one enclosing type. In our case, this is possible if one of the types is a subtype of `Real`, then the enclosing type is `Hyperbolic`.

After adding methods for `promote_rule`, it becomes possible to use functions `promote`, `promote_type` and `convert`:

```
>>h = Hyperbolic(1 // 2)
>>promote(h, 1)
(1//2+0//1j, 1//1+0//1j)
>>promote_type(Hyperbolic{Int64}, Float32)
Hyperbolic{Float32}
```

The first function is already familiar to us. The second allows you to infer the enclosing type not of specific variable values, but of the types themselves. A type in Julia is an object of the first kind (type `DataType`) and can be assigned to other variables, passed as function arguments, and so on.

Function `convert` allows you to convert the type specific value, for example:

```
>>convert(Hyperbolic, 1)
1+0j
```

After adding methods for type casting, you can start adding methods for arithmetic operations. A feature of Julia is the implementation of arithmetic operations not in the form of operators, but in the form of functions. For example, the following calls are correct:

```
>>+(1,2)
3
>>+(1,2,3,4)
10
>>+((i for i in 1:10)...)
55
```

In this regard, adding methods for arithmetic operations is no different from the corresponding process for other functions.

Adding methods for unary operations `+` and `-` is carried out as follows:

```
Base.:+(h::Hyperbolic) = Hyperbolic(+h.re, +h.jm)
Base.:-(h::Hyperbolic) = Hyperbolic(-h.re, -h.jm)
```

This is an abbreviated function declaration.

Similarly, methods are added for binary addition, subtraction, multiplication, and division. Here is the code for addition and multiplication:

```
# Binary + and *
function Base.+(x::Hyperbolic, y::Hyperbolic)
    xx = x.re + y.re
    yy = x.jm + y.jm
    Hyperbolic(xx, yy)
end
function Base.*(x::Hyperbolic, y::Hyperbolic)
    xx = x.re * y.re + x.jm * y.jm
    yy = x.re * y.jm + x.je * y.re
    return Hyperbolic(xx, yy)
end
```

5. Conclusion

We examined the mechanism of multiple dispatch underlying the Julia language, using the example of the implementation of hyperbolic numbers. This example allowed us to touch upon such concepts of the language as the hierarchy of data types, composite data types, type casting mechanisms, function overloading (creating new methods for functions in terms of the Julia language), etc.

Acknowledgments

This paper has been supported by the RUDN University Strategic Academic Leadership Program.

References

- [1] J. Bezanson, A. Edelman, S. Karpinski, and V. B. Shah, “Julia: A fresh approach to numerical computing,” *SIAM Review*, vol. 59, no. 1, pp. 65–98, Jan. 2017. DOI: 10.1137/141000671.
- [2] M. N. Gevorkyan, D. S. Kulyabov, and L. A. Sevastyanov, “Review of Julia programming language for scientific computing,” in *The 6th International Conference “Distributed Computing and Grid-technologies in Science and Education”*, 2014, p. 27.
- [3] T. E. Oliphant, *Guide to NumPy*, 2nd. CreateSpace Independent Publishing Platform, 2015.
- [4] F. Zappa Nardelli, J. Belyakova, A. Pelenitsyn, B. Chung, J. Bezanson, and J. Vitek, “Julia subtyping: a rational reconstruction,” *Proceedings of the ACM on Programming Languages*, vol. 2, no. OOPSLA, pp. 1–27, Oct. 2018. DOI: 10.1145/3276483.
- [5] K. Driesen, U. Hözlze, and J. Vitek, “Message dispatch on pipelined processors,” in *ECOOP’95 — Object-Oriented Programming, 9th European Conference, Aarhus, Denmark, August 7–11, 1995* (Lecture Notes in Computer Science), M. Tokoro and R. Pareschi, Eds., Lecture Notes in Computer Science. Springer Berlin Heidelberg, 1995, vol. 952. DOI: 10.1007/3-540-49538-x_13.

- [6] R. Muschevici, A. Potanin, E. Tempero, and J. Noble, "Multiple dispatch in practice," in *OOPSLA'08: Proceedings of the 23rd ACM SIGPLAN conference on Object-oriented programming systems languages and applications*, ACM Press, Oct. 2008, pp. 563–582. DOI: 10.1145/1449764.1449808.
- [7] S. Gowda, Y. Ma, A. Cheli, M. Gwózzdź, V. B. Shah, A. Edelman, and C. Rackauckas, "High-performance symbolic-numeric via multiple dispatch," *ACM Communications in Computer Algebra*, vol. 55, no. 3, pp. 92–96, Jan. 2022. DOI: 10.1145/3511528.3511535.
- [8] I. M. Yaglom, *Complex numbers in Geometry*. Academic Press, 1968, 243 pp.
- [9] I. M. Yaglom, B. A. Rozenfel'd, and E. U. Yasinskaya, "Projective metrics," *Russian Mathematical Surveys*, vol. 19, no. 5, pp. 49–107, Oct. 1964. DOI: 10.1070/RM1964v019n05ABEH001159.
- [10] D. S. Kulyabov, A. V. Korolkova, and L. A. Sevastianov, *Complex numbers for relativistic operations*, Dec. 2021. DOI: 10.20944/preprints202112.0094.v1.
- [11] D. S. Kulyabov, A. V. Korolkova, and M. N. Gevorkyan, "Hyperbolic numbers as Einstein numbers," *Journal of Physics: Conference Series*, vol. 1557, 012027, pp. 012027.1–5, May 2020. DOI: 10.1088/1742-6596/1557/1/012027.
- [12] P. Fjelstad, "Extending special relativity via the perplex numbers," *American Journal of Physics*, vol. 54, no. 5, pp. 416–422, May 1986. DOI: 10.1119/1.14605.
- [13] W. Band, "Comments on extending relativity via the perplex numbers," *American Journal of Physics*, vol. 56, no. 5, pp. 469–469, May 1988. DOI: 10.1119/1.15582.
- [14] J. Rooney, "On the three types of complex number and planar transformations," *Environment and Planning B: Planning and Design*, vol. 5, no. 1, pp. 89–99, 1978. DOI: 10.1068/b050089.
- [15] J. Rooney, "Generalised complex numbers in Mechanics," in *Advances on Theory and Practice of Robots and Manipulators*, ser. Mechanisms and Machine Science, M. Ceccarelli and V. A. Glazunov, Eds., vol. 22, Cham: Springer International Publishing, 2014, pp. 55–62. DOI: 10.1007/978-3-319-07058-2_7.
- [16] M. N. Gevorkyan, A. V. Korolkova, and D. S. Kulyabov, "Approaches to the implementation of generalized complex numbers in the Julia language," in *Workshop on information technology and scientific computing in the framework of the X International Conference Information and Telecommunication Technologies and Mathematical Modeling of High-Tech Systems (ITTMM-2020)*, ser. CEUR Workshop Proceedings, vol. 2639, Aachen, Apr. 2020, pp. 141–157.

For citation:

A. V. Korolkova, M. N. Gevorkyan, D. S. Kulyabov, Implementation of hyperbolic complex numbers in Julia language, *Discrete and Continuous Models and*

Applied Computational Science 30 (4) (2022) 318–329. DOI: 10.22363/2658-4670-2022-30-4-318-329.

Information about the authors:

Korolkova, Anna V. — Docent, Candidate of Sciences in Physics and Mathematics, Associate Professor of Department of Applied Probability and Informatics of Peoples' Friendship University of Russia (RUDN University) (e-mail: korolkova-av@rudn.ru, phone: +7(495) 952-02-50, ORCID: <https://orcid.org/0000-0001-7141-7610>)

Gevorkyan, Migran N. — Candidate of Sciences in Physics and Mathematics, Assistant Professor of Department of Applied Probability and Informatics of Peoples' Friendship University of Russia (RUDN University) (e-mail: gevorgyan-mn@rudn.ru, phone: +7 (495) 955-09-27, ORCID: <https://orcid.org/0000-0002-4834-4895>)

Kulyabov, Dmitry S. — Professor, Doctor of Sciences in Physics and Mathematics, Professor at the Department of Applied Probability and Informatics of Peoples' Friendship University of Russia (RUDN University) (e-mail: kulyabov-ds@rudn.ru, phone: +7 (495) 952-02-50, ORCID: <https://orcid.org/0000-0002-0877-7063>)

УДК 511.14:004.432

DOI: 10.22363/2658-4670-2022-30-4-318-329

Реализация гиперболических комплексных чисел на языке Julia

А. В. Королькова¹, М. Н. Геворкян¹, Д. С. Кулябов^{1,2}

¹ *Российский университет дружбы народов,
ул. Миклухо-Маклая, д. 6, Москва, 117198, Россия*

² *Объединённый институт ядерных исследований,
ул. Жолио-Кюри 6, Дубна, Московская область, 141980, Россия*

Аннотация. Гиперболические комплексные числа применяются при описании гиперболических пространств. Одним из известных примеров таких пространств является пространство Минковского, играющее ведущее значение в задачах частной теории относительности, электродинамики. Однако такие числа не очень распространены в разных языках программирования. Представляет интерес реализация гиперболических комплексных чисел в языках научного программирования, в частности в языке Julia. В основе языка Julia лежит концепция множественной диспетчеризации (multiple dispatch). Эта концепция является расширением концепции полиморфизма для объектно-ориентированных языков программирования. Разработана библиотека для Julia, реализующая гиперболические комплексные числа. По результатам исследования можно сделать вывод об удобстве и естественности концепции множественной диспетчеризации в языках научного программирования.

Ключевые слова: язык программирования Julia, множественная диспетчеризация, абстрактные типы данных, конвертация типов, параметрические структуры, гиперболические комплексные числа



UDC 517.958:621.372.8

PACS 07.05.Tp, 02.60.Pn, 02.70.Bf

DOI: 10.22363/2658-4670-2022-30-4-330-341

On a dispersion curve of a waveguide filled with inhomogeneous substance

Oleg K. Kroytor¹, Mikhail D. Malykh^{1,2}

¹ Peoples' Friendship University of Russia (RUDN University),
6, Miklukho-Maklaya St., Moscow, 117198, Russian Federation

² Meshcheryakov Laboratory of Information Technologies,
Joint Institute for Nuclear Research,
6, Joliot-Curie St., Dubna, Moscow Region, 141980, Russian Federation

(received: October 26, 2022; revised: December 8, 2022; accepted: December 19, 2022)

Abstract. The paper discusses the relationship between the modes traveling along the axis of the waveguide and the standing modes of a cylindrical resonator, and shows how this relationship can be explored using the Sage computer algebra system. In this paper, we study this connection and, on its basis, describe a new method for constructing the dispersion curve of a waveguide with an optically inhomogeneous filling. The aim of our work was to find out what computer algebra systems can give when calculating the points of the waveguide dispersion curve. Our method for constructing the dispersion curve of a waveguide with optically inhomogeneous filling differs from those proposed earlier in that it reduces this problem to calculating the eigenvalues of a self-adjoint matrix, i.e., a well-studied problem. The use of a self-adjoint matrix eliminates the occurrence of artifacts associated with the appearance of a small imaginary addition to the eigenvalues. We have composed a program in the Sage computer algebra system that implements this method for a rectangular waveguide with rectangular inserts and tested it on SLE modes. The obtained results showed that the program successfully copes with the calculation of the points of the dispersion curve corresponding to the hybrid modes of the waveguide, and the points found fit the analytical curve with graphical accuracy even when with a small number of basis elements taken into account.

Key words and phrases: waveguide, Maxwell's equations, normal modes, partial radiation conditions

1. Introduction

In classical electrodynamics, there are two related spectral problems — the problem of the normal modes of the waveguide and the problem of eigenmodes of the resonator. Recall their formulations.

© Kroytor O. K., Malykh M. D., 2022



This work is licensed under a Creative Commons Attribution 4.0 International License

<https://creativecommons.org/licenses/by-nc/4.0/legalcode>

Let G be a regular domain in \mathbb{R}^3 , below referred to as a resonator. A non-trivial field of the form

$$\vec{E} = \vec{E}(x, y, z)e^{i\omega t}, \quad \vec{H} = \vec{H}(x, y, z)e^{i\omega t},$$

satisfying the system of homogeneous Maxwell equations and boundary conditions

$$\vec{n} \times \vec{E} = 0, \quad \vec{n} \cdot \vec{H} = 0,$$

is called the eigenmode, and the corresponding value of the positive parameter ω is called the eigenfrequency, instead of which the wave number $k = \omega/c$ is usually used. To find the eigenfrequencies, it is necessary to solve the eigenvalue problem

$$\text{rot}\vec{E} = -ik\mu\vec{H}, \quad \text{rot}\vec{H} = ik\epsilon\vec{E}$$

with the boundary conditions

$$\vec{n} \times \vec{E} = 0, \quad \vec{n} \cdot \vec{H} = 0.$$

This problem, like the scalar one, is written as an eigenvalue problem for a completely continuous self-adjoint operator, and therefore it has a discrete spectrum, which can be found approximately using the Ritz method [1, p. 181]. To theoretically substantiate this statement, special Sobolev spaces are introduced, the embedding theorems for which, unfortunately, have so far been proved under the assumption of a smooth boundary [2, § 6.1].

Let S be a regular domain in \mathbb{R}^2 , let us call the cylinder $S \times \mathbb{R}$ a waveguide. Assume that the axis Oz of the used Cartesian coordinate system is directed along the axis of the cylinder. A non-trivial field of the form

$$\vec{E} = \vec{E}(x, y)e^{i\omega t - i\gamma z}, \quad \vec{H} = \vec{H}(x, y)e^{i\omega t - i\gamma z},$$

satisfying the system of homogeneous Maxwell equations and boundary conditions

$$\vec{n} \times \vec{E} = 0, \quad \vec{n} \cdot \vec{H} = 0,$$

is called the normal waveguide mode [3]. In this case, the parameter $\beta = \gamma/c$ is called the phase constant. To find it at a fixed frequency, it is required to solve the eigenvalue problem

$$\overline{\text{rot}}\vec{E} = -ik\mu\vec{H}, \quad \overline{\text{rot}}\vec{H} = ik\epsilon\vec{E}$$

with the boundary conditions

$$\vec{n} \times \vec{E} = 0, \quad \vec{n} \cdot \vec{H} = 0.$$

Here, $\overline{\text{rot}}$ means a differential operator in which differentiation with respect to z is replaced with multiplication by $-i\gamma$. The points of the $k\gamma$ plane, at which this problem has a nontrivial solution, form a certain curve called the waveguide dispersion curve.

The spectral problem for waveguide modes does not belong to any studied type. In the case when the filling of the waveguide is homogeneous, the

complete system of waveguide modes can be composed of two types of modes: transverse magnetic ($H_z = 0$) and transverse electric ($E_z = 0$) ones. The Borgnis theory of functions makes it possible to reduce the study of such modes to the study of the Laplace operator spectrum. In this case, the dispersion curve turns out to be the union of a countable number of hyperbolas [3, 4].

Traditionally, this problem is written as an eigenvalue problem with respect to three field components. The choice of the three field components from the six components of the vectors \vec{E} and \vec{H} can be done in different ways, which leads to different formulations of the problem. A. N. Bogolyubov and T. V. Edakina [5, 6] and Frank Schmidt [7, 8] used the components of vector \vec{H} , in the papers by E. Lezar and D. Davidson [9] vector \vec{E} was used, A. L. Delitsyn [10–13] formulated the problem in terms of H_x, H_y, E_z . Normal modes of an axially symmetric waveguide with a dielectric core were considered by N. A. Novoselova, S. B. Raevsky and A. A. Titarenko [14], as well as by A. L. Delitsyn and S. I. Kruglov [15]. Potentials can be used instead of fields, for example, four scalar functions, as proposed in Refs. [16–18]. Finally, with considerable efforts, it is possible to reduce the spectral problem to the study of the spectrum of a self-adjoint quadratic pencil [19].

Traditionally, the spectral problem of the theory of waveguides was considered as an eigenvalue problem with respect to the parameter γ , and the wave number was considered given. This approach is justified, since the problem of waveguide diffraction considers the incidence of a monochromatic wave, which partially passes through and is partially reflected from the inhomogeneity; in this case, transmitted and reflected waves arise, travelling from the inhomogeneity, but having the same frequency as the incident wave. On the other hand, to construct a dispersion curve, it is quite unnecessary to calculate its points at a sequence of frequency values. It is possible to search for its points at fixed values of γ . What is of importance here is only the convenience of solving the problem.

It is obvious from physical considerations that there should be a simple relationship between the modes traveling along the waveguide axis and the standing modes of the cylindrical resonator. In this paper, we investigate this relationship and, based on it, describe a new method for constructing the dispersion curve of a waveguide with an optically inhomogeneous filling.

2. Relation between travelling and standing modes

We managed to express the relation between the travelling and standing modes by two theorems.

Theorem 1. *If the waveguide $S \times \mathbb{R}$ has a normal mode*

$$\vec{E} = \vec{E}(x, y)e^{i\omega t - i\gamma z}, \quad \vec{H} = \vec{H}(x, y)e^{i\omega t - i\gamma z}$$

at certain values of ω, γ , then the resonator $S \times [0, \pi n/\gamma]$ has an eigenmode at the same ω, γ .

Theorem 2. *If the resonator $S \times [0, L]$ has an eigenmode*

$$\vec{E} = \vec{E}(x, y, z)e^{i\omega t}, \quad \vec{H} = \vec{H}(x, y, z)e^{i\omega t}$$

whose components have continuous derivatives at $z = 0, L$, then it also has an eigenmode

$$\begin{aligned} E_{x,y} &= E_{x,y}(x, y) \sin \frac{\pi n z}{L} e^{i\omega t}, & E_z &= E_z(x, y) \cos \frac{\pi n z}{L} e^{i\omega_s t}, \\ H_{x,y} &= H_{x,y}(x, y) \cos \frac{\pi n z}{L} e^{i\omega t}, & H_z &= H_z(x, y) \sin \frac{\pi n z}{L} e^{i\omega t}, \end{aligned}$$

for some natural value n , and the waveguide $S \times \mathbb{R}$ has a normal mode at the same frequency ω and $\gamma = \pi n/L$.

Proven theorems allow us to reduce the solution of the spectral problem of the theory of waveguides to the solution of the spectral problem of the theory of cylindrical resonators.

3. Eigenmodes of resonators

Let G be a resonator filled with a substance characterized, generally speaking, by variable ϵ and constant μ . In this case, it is convenient to exclude \vec{E} from the system of Maxwell equations and write down the system of second-order equations

$$\operatorname{rot} \frac{1}{\epsilon} \operatorname{rot} \vec{H} = k^2 \mu \vec{H}, \tag{1}$$

to which the boundary conditions should be added

$$\vec{H} \cdot \vec{n} = 0, \quad \operatorname{rot} \vec{H} \times \vec{n} = 0 \tag{2}$$

Every non-trivial solution \vec{H} of the problem (1), (2) has an eigenmode

$$\vec{E} = \frac{1}{ik\epsilon} \operatorname{rot} H e^{i\omega t}, \quad \vec{H} = \vec{H} e^{i\omega t}$$

of the resonator G . Let us multiply (1) by the test vector \vec{F} , integrate over G and apply the integration by parts:

$$\iiint_G \operatorname{rot} \vec{F}^* \cdot \operatorname{rot} \vec{H} \frac{dxdydz}{\epsilon} - k^2 \mu \iiint_G \vec{F}^* \cdot \vec{H} dxdydz = 0. \tag{3}$$

The closure of the set of vectors $\vec{F} \in C^1(\overline{G})$ satisfying the condition $\operatorname{div} \vec{F} = 0$ in G and $\vec{F} \cdot n = 0$ on its boundary, in the norm generated by the scalar product

$$(\vec{F}, \vec{H}) = \iiint_G \operatorname{rot} \vec{F}^* \cdot \operatorname{rot} \vec{H} \frac{dxdydz}{\epsilon} + \mu \iiint_G \vec{F}^* \cdot \vec{H} dxdydz,$$

is a Hilbert space, which we will denote as $\mathfrak{H}(G)$. The generalized eigenmode of the resonator G is the nonzero vector $\vec{H} \in \mathfrak{H}(G)$ that satisfies the identity (3) for any vector $\vec{F} \in \mathfrak{H}(G)$.

It follows from the embedding theorem [2] that there exists a completely continuous self-adjoint operator \hat{A} such that

$$\mu \iiint_G \vec{F}^* \cdot \vec{H} dx dy dz = \iiint_G \text{rot} \vec{F}^* \cdot \text{rot}(\hat{A} \vec{H}) \frac{dx dy dz}{\epsilon}.$$

Therefore, the relation (3) can be written as $\vec{H} = k^2 \hat{A} \vec{H}$.

Hence, the eigenfrequencies of the resonator form an infinitely large sequence, and the eigenmodes corresponding to them form an orthonormal basis in the space $\mathfrak{H}(G)$.

The eigenvalues of a self-adjoint, completely continuous operator can be found using the Ritz method, it is only necessary to choose the basis of the space $\mathfrak{H}(G)$ in a proper way.

4. Dispersion curve of a waveguide

Let us consider the points of intersection of the waveguide dispersion curve $S \times \mathbb{R}$ with the straight line $\gamma = \text{const}$. Each such point corresponds to the normal mode of the waveguide, and, by virtue of theorem 1, to the eigenmode of the resonator $S \times [0, \pi/\gamma]$. The eigenfrequencies of this resonator form an infinite monotonic sequence $\omega_1, \omega_2, \dots$. By virtue of theorem 2, these points correspond to modes from which one can construct normal waveguide modes. From here a theorem immediately follows.

Theorem 3. *The points of intersection of the waveguide dispersion curve $S \times \mathbb{R}$ with the straight line $\gamma = \text{const}$ form a countable set of points, whose set of abscissas coincides with the set of the resonator eigenfrequencies $S \times [0, \pi/\gamma]$.*

Thus, in order to construct a dispersion curve, it is necessary to solve the self-adjoint problem of natural vibrations of a cylindrical resonator G using the Ritz method. The choice of a basis is complicated by the fact that the elements of the space $\mathfrak{H}(G)$ must satisfy the condition $\text{div} \vec{F} = 0$.

To construct such a basis, we took the eigenfunctions ϕ_n of the Dirichlet problem on the section of a cylinder

$$\Delta_2 \phi + \alpha^2 \phi = 0, \quad \phi|_{\partial S} = 0$$

and eigenfunctions ψ_n of the Neumann problem on the section of a cylinder

$$\Delta_2 \psi + \beta^2 \psi = 0, \quad \left. \frac{\partial \psi}{\partial n} \right|_{\partial S} = 0.$$

We will take orthonormal systems ϕ_n and ψ_n with respect to $L^2(S)$. With their help, we construct the basis formed by TM fields

$$\vec{H} = \begin{pmatrix} \partial_y \phi_n(x, y) \\ -\partial_x \phi_n(x, y) \\ 0 \end{pmatrix} \cos s\gamma z, \quad n, m \in \mathbb{N},$$

and another basis for the TE fields

$$\vec{H} = \begin{pmatrix} \gamma \partial_x \psi_n(x, y) \cos s\gamma z \\ \gamma \partial_y \psi_n(x, y) \cos s\gamma z \\ \beta_n^2 \psi_n(x, y) \sin s\gamma z \end{pmatrix}, \quad n \in \mathbb{N}, m \in \mathbb{Z}, m \geq 0,$$

where $\gamma = \pi/L$, and s takes integer values, but for our case when ϵ is independent of z , it is sufficient to take $s = 1$.

Truncating the infinite system to the first N basis functions, we reduce the problem of finding the wave numbers (3) to an algebraic eigenvalue problem

$$\hat{A}H = k^2 \hat{B}H. \tag{4}$$

If we agree to write the first N TM waves, and then the first N TE waves, then the matrices of this system will have a block form

$$\hat{A} = \begin{pmatrix} A_{11}, & A_{12} \\ A_{21}, & A_{22} \end{pmatrix}, \quad \hat{B} = \begin{pmatrix} B_{11}, & 0 \\ 0, & B_{22} \end{pmatrix}.$$

We composed the matrix elements as integrals over a cylinder and took those integrals that could be calculated explicitly for $\epsilon(x, y)$. The matrix \hat{B} turned out to be diagonal, and

$$B_{11} = \text{diag} \left(\frac{\alpha_n^2 \mu}{2} \right), \quad B_{22} = \text{diag} \left(\frac{\beta_n^2 \mu}{2} (\gamma^2 + \beta_n^2) \right).$$

Therefore, the generalized eigenvalue problem (4) is reduced to the standard eigenvalue problem:

$$\hat{D}\vec{H} = k^2 \vec{H}.$$

The elements of the symmetric matrix \hat{D} are defined as double integrals:

$$d_{n,m} = \frac{\gamma^2}{\alpha_n \alpha_m} \iint_S (\nabla \phi_n \cdot \nabla \phi_m) \frac{dx dy}{\epsilon \mu} + \alpha_n \alpha_m \iint_S \phi_n \phi_m \frac{dx dy}{\epsilon \mu},$$

$n, m = 1, \dots, N_1,$

$$d_{n,m} = \frac{\gamma}{\alpha_n \beta_m} \sqrt{\beta_m^2 + \gamma^2} \iint_S \frac{\partial \psi_m \phi_n}{\partial xy} \frac{dx dy}{\epsilon \mu},$$

$n = 1, \dots, N_1, m = N_1 + 1, \dots, N_1 + N_2,$

$$d_{n,m} = \frac{1}{\beta_n \beta_m} \sqrt{\beta_m^2 + \gamma^2} \sqrt{\beta_n^2 + \gamma^2} \iint_S \nabla \psi_n \cdot \nabla \psi_m \frac{dx dy}{\epsilon \mu},$$

$n, m = N_1 + 1, \dots, N_1 + N_2.$

5. Calculation of the points of the waveguide dispersion curve in the Sage system

As is usually the case when applying the Ritz method, the matrix elements are integrals, which in the general case are calculated approximately. To avoid this problem in the first tests, we considered a special case when all integrals are calculated in elementary functions.

Consider a rectangular waveguide $S = L_x \times L_y$ with uniform filling $\epsilon_0 = 1$ and $\mu = 1$ (see figure 1). Inside it we place a rectangular insert S_1 with constant filling ϵ_1 and $\mu = 1$. In this case, ϕ_n and ψ_n are products of sines and cosines, and the matrix elements are integrals of such products over rectangular regions.

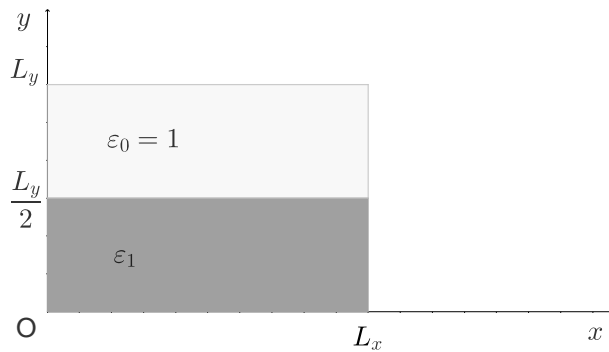


Figure 1. Waveguide cross section

We compiled a program (<https://github.com/malykhmd>) in the Sage computer algebra system that calculates these integrals in symbolic form, composes the \hat{D} matrix for any given numerical value of γ , and calculates its eigenvalues using the standard `linalg` library function.

To test this program, we considered a waveguide in which the insert occupies the bottom half (see figure 1). In this case, two families of normal modes can be written analytically: SLE and SLH modes [4]. This example is interesting because these modes are hybrid and cannot be found by methods that ignore this effect.

Figures 2, 3, and 4 demonstrate the results of analytical and numerical calculations performed using our program. It is clearly seen that for lower modes, the points found by our program fit the analytical curve with graphical accuracy even when a very small number of basis elements are taken into account (three for each direction). This is not hindered by the proximity of the neighboring arc due to the close values of ϵ_0 and ϵ_1 . The accuracy of the calculations decreases with the growth of ϵ_1 , but when using 10 modes the calculated points fit the analytical curve even at $\epsilon_1 = 2$ (see figure 4).

The obtained results showed that the program successfully copes with the calculation of the points of the dispersion curve corresponding to the hybrid modes of the waveguide, and the points found fit the analytical curve with graphical accuracy even when with a small number of basis elements taken into account.

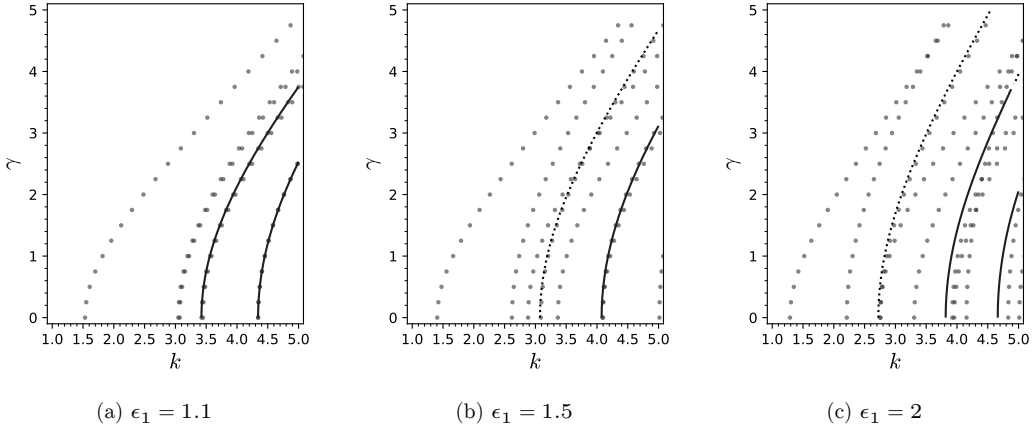


Figure 2. Dispersion curve of a waveguide with an insert at $L_x = 1, L_y = 2$. The dots indicate the points of the dispersion curve found numerically (3 modes were taken in each of the directions), the solid lines are arcs of the dispersion curve corresponding to the SLE modes

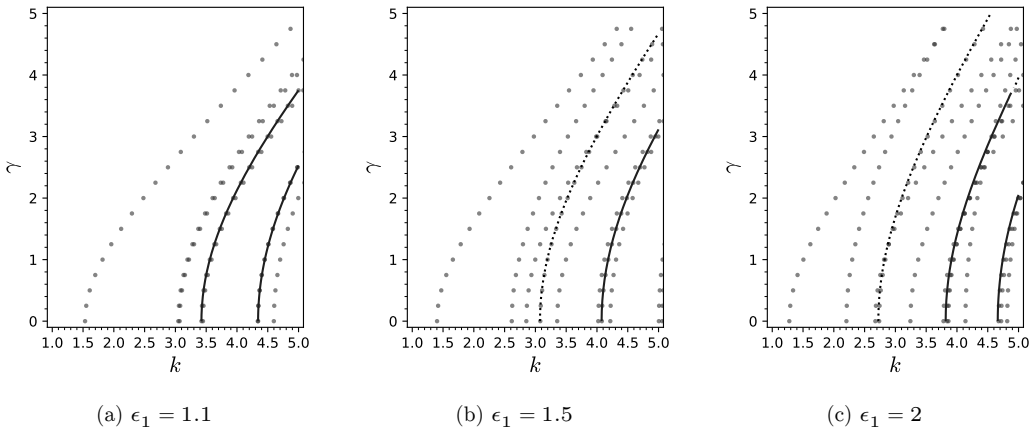


Figure 3. Dispersion curve of a waveguide with an insert at $L_x = 1, L_y = 2$. The dots indicate the points of the dispersion curve found numerically (6 modes are taken in each of the directions), the solid lines are arcs of the dispersion curve corresponding to the SLE modes

6. Conclusion

Our approach to constructing the dispersion curve of a waveguide with an optically inhomogeneous filling differs from those proposed earlier in that it reduces the problem to calculating eigenvalues of a self-adjoint matrix, i.e., a well-studied problem. The use of a self-adjoint matrix eliminates the occurrence of artifacts associated with the appearance of a small imaginary addition to the eigenvalues.

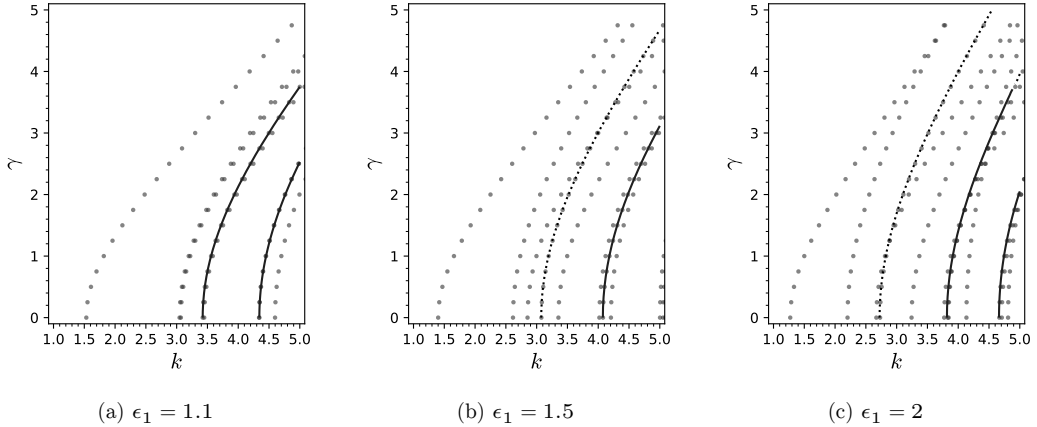


Figure 4. Dispersion curve of a waveguide with an insert at $L_x = 1$, $L_y = 2$. The dots indicate the points of the dispersion curve found numerically (10 modes were taken in each of the directions), the solid lines are arcs of the dispersion curve corresponding to the SLE modes

We implemented this approach for an example of a rectangular waveguide with rectangular inserts in the Sage computer algebra system and tested it using SLE modes. At the same time, it was shown that our program perfectly copes with calculating the points of the dispersion curve corresponding to the hybrid modes of the waveguide.

Acknowledgments

This work is supported by the Russian Science Foundation (grant no. 20-11-20257).

References

- [1] M. M. Karliner, *Microwave electrodynamics: Lecture course [Elektrodinamika SVCH: Kurs lektsiy]*. Novosibirsk: Novosibirsk state university, 2006, In Russian.
- [2] G. Duvaut and J. L. Lions, *Les inéquations en mécanique et en physique*. Paris: Dunod, 1972.
- [3] I. E. Mogilevsky and A. G. Sveshnikov, *Mathematical problems of diffraction theory [Matematicheskiye zadachi teorii difraktsii]*. Moscow: MSU, 2010, In Russian.
- [4] W. C. Chew, *Lectures on theory of microwave and optical waveguides*. 2012. DOI: 10.48550/arXiv.2107.09672.

- [5] A. N. Bogolyubov and T. V. Edakina, "Application of variation-difference methods for calculation of dielectric waveguides [Primeneniye variatsionno-raznostnykh metodov dlya rascheta dielektricheskikh volnovodov]," *Bulletin of Moscow University. Series 3: Physics. Astronomy*, vol. 32, no. 2, pp. 6–14, 1991, In Russian.
- [6] A. N. Bogolyubov and T. V. Edakina, "Calculation of dielectric waveguides with complex cross-section shape by variation-difference method [Raschet dielektricheskikh volnovodov so slozhnoy formoy poperechnogo secheniya variatsionno-raznostnym metodom]," *Bulletin of Moscow University. Series 3: Physics. Astronomy*, vol. 34, no. 3, pp. 72–74, 1992, In Russian.
- [7] P. Deuffhard, F. Schmidt, T. Friese, and L. Zschiedrich, "Adaptive Multigrid Methods for the Vectorial Maxwell Eigenvalue Problem for Optical Waveguide Design," in *Mathematics — Key Technology for the Future*, W. Jäger and H. J. Krebs, Eds., Berlin–Heidelberg: Springer, 2011, pp. 279–292. DOI: 10.1007/978-3-642-55753-8_23.
- [8] F. Schmidt, S. Burger, J. Pomplun, and L. Zschiedrich, "Advanced FEM analysis of optical waveguides: algorithms and applications," *Proc. SPIE*, vol. 6896, 2008. DOI: 10.1117/12.765720.
- [9] E. Lezar and D. B. Davidson, "Electromagnetic waveguide analysis," in *Automated solution of differential equations by the finite element method*, The FEniCS Project, 2011, pp. 629–643.
- [10] A. N. Bogolyubov, A. L. Delitsyn, and A. G. Sveshnikov, "On the completeness of the set of eigen- and associated functions of a waveguide [O polnote sistemy sobstvennykh i prisoyedinennykh funktsiy volnovoda]," *Computational Mathematics and Mathematical Physics*, vol. 38, no. 11, pp. 1815–1823, 1998, In Russian.
- [11] A. N. Bogolyubov, A. L. Delitsyn, and A. G. Sveshnikov, "On the problem of excitation of a waveguide filled with an inhomogeneous medium [O zadache возбужdeniya volnovoda s neodnorodnym zapolneniyem]," *Computational Mathematics and Mathematical Physics*, vol. 39, no. 11, pp. 1794–1813, 1999, In Russian.
- [12] A. L. Delitsyn, "An approach to the completeness of normal waves in a waveguide with magnetodielectric filling," *Differential Equations*, vol. 36, no. 5, pp. 695–700, 2000. DOI: 10.1007/BF02754228.
- [13] A. L. Delitsyn, "On the completeness of the system of eigenvectors of electromagnetic waveguides," *Computational Mathematics and Mathematical Physics*, vol. 51, no. 10, pp. 1771–1776, 2011. DOI: 10.1134/S0965542511100058.
- [14] N. A. Novoselova, S. B. Raevsky, and A. A. Titarenko, "Calculation of propagation characteristics of symmetrical waves of round waveguide with radial non-uniform dielectric filling [Raschet kharakteristik rasprostraneniya simmetrichnykh voln kruglogo volnovoda s radial'no-neodnorodnym dielektricheskim zapolneniyem]," *Proceedings of Nizhny Novgorod State Technical University named after R.E. Alekseev*, vol. 2, no. 81, pp. 30–38, 2010, In Russian.

- [15] A. L. Delitsyn and S. I. Kruglov, “Mixed finite elements used to analyze the real and complex modes of cylindrical waveguides,” *Moscow University Physics Bulletin*, vol. 66, no. 6, pp. 546–551, 2011. DOI: 10.3103/S0027134911060063.
- [16] A. A. Tiutiunnik, D. V. Divakov, M. D. Malykh, and L. A. Sevast’yanov, “Symbolic-Numeric Implementation of the Four Potential Method for Calculating Normal Modes: An Example of Square Electromagnetic Waveguide with Rectangular Insert,” *Lecture notes in computer science*, vol. 11661, pp. 412–429, 2019. DOI: 10.1007/978-3-030-26831-2_27.
- [17] D. V. Divakov, M. D. Malykh, L. A. Sevast’yanov, and A. A. Tiutiunnik, “On the Calculation of Electromagnetic Fields in Closed Waveguides with Inhomogeneous Filling,” *Lecture notes in computer science*, vol. 11189, pp. 458–465, 2019. DOI: 10.1007/978-3-030-10692-8_52.
- [18] M. D. Malykh and L. A. Sevast’yanov, “On the representation of electromagnetic fields in discontinuously filled closed waveguides by means of continuous potentials,” *Computational Mathematics and Mathematical Physics*, vol. 59, no. 2, pp. 330–342, 2019. DOI: 10.1134/S0965542519020118.
- [19] O. K. Kroytor, M. D. Malykh, and L. A. Sevast’yanov, “On normal modes of a waveguide,” *Computational Mathematics and Mathematical Physics*, vol. 62, no. 3, pp. 393–410, 2022. DOI: 10.1134/S0965542522030083.

For citation:

O. K. Kroytor, M. D. Malykh, On a dispersion curve of a waveguide filled with inhomogeneous substance, *Discrete and Continuous Models and Applied Computational Science* 30 (4) (2022) 330–341. DOI: 10.22363/2658-4670-2022-30-4-330-341.

Information about the authors:

Kroytor, Oleg K. — Senior lecturer of Department of Applied Probability and Informatics of Peoples’ Friendship University of Russia (RUDN University) (e-mail: kroytor-ok@rudn.ru, phone: +7(495)9550927, ORCID: <https://orcid.org/0000-0002-5691-7331>)

Malykh, Mikhail D. — Doctor of Physical and Mathematical Sciences, Assistant Professor of Department of Applied Probability and Informatics of Peoples’ Friendship University of Russia (RUDN University) (e-mail: malykh-md@rudn.ru, phone: +7(495)9550927, ORCID: <https://orcid.org/0000-0001-6541-6603>, ResearcherID: P-8123-2016, Scopus Author ID: 6602318510)

УДК 517.958:621.372.8

PACS 07.05.Tr, 02.60.Pn, 02.70.Bf

DOI: 10.22363/2658-4670-2022-30-4-330-341

О дисперсионной кривой волновода, заполненного неоднородным веществом

О. К. Кройтор¹, М. Д. Малых^{1,2}

¹ *Российский университет дружбы народов,
ул. Миклухо-Маклая, д. 6, Москва, 117198, Россия*

² *Лаборатория информационных технологий им. М. Г. Мецеракова,
Объединённый институт ядерных исследований,
ул. Жолио-Кюри, д. 6, Дубна, Московская область, 141980, Россия*

Аннотация. В статье рассматривается связь между модами, бегущими вдоль оси волновода, и стоячими модами цилиндрического резонатора. Показывается, как данная связь может быть исследована с помощью системы компьютерной алгебры Sage. В работе мы исследуем эту связь и на её основе описываем новый метод построения дисперсионной кривой волновода с оптически неоднородным заполнением. Целью нашей работы было выяснить, что могут дать системы компьютерной алгебры при вычислении (точек) дисперсионной кривой волновода. Метод построения дисперсионной кривой волновода с оптически неоднородным заполнением, предложенный нами, отличается от предложенных ранее тем, что сводит эту задачу к вычислению собственных значений самосопряжённой матрицы, то есть к задаче, хорошо изученной. Использование самосопряжённой матрицы исключает возникновение артефактов, связанных с появлением малой мнимой добавки у собственных значений. Мы составили программу в системе компьютерной алгебры Sage, в которой реализован этот метод для волновода прямоугольного сечения с прямоугольными вставками, и протестировали её на SLE-модах. Полученные результаты показали, что программа успешно справляется с вычислением точек дисперсионной кривой, отвечающих гибридным модам волновода, и найденные точки с графической точностью ложатся на аналитическую кривую даже при небольшом числе учитываемых базисных элементов.

Ключевые слова: волновод, уравнения Максвелла, нормальные моды, частичные условия излучения



UDC 519.6

PACS 07.05.Tp, 02.60.Pn, 02.70.Bf

DOI: 10.22363/2658-4670-2022-30-4-342-356

On a modification of the Hamming method for summing discrete Fourier series and its application to solve the problem of correction of thermographic images

Evgeniy B. Laneev, Obaida Baaj

*Peoples' Friendship University of Russia (RUDN University),
6, Miklukho-Maklaya St., Moscow, 117198, Russian Federation*

(received: August 31, 2022; revised: December 12, 2022; accepted: December 19, 2022)

Abstract. The paper considers mathematical methods of correction of thermographic images (thermograms) in the form of temperature distribution on the surface of the object under study, obtained using a thermal imager. The thermogram reproduces the image of the heat-generating structures located inside the object under study. This image is transmitted with distortions, since the sources are usually removed from its surface and the temperature distribution on the surface of the object transmits the image as blurred due to the processes of thermal conductivity and heat exchange. In this paper, the continuation of the temperature function as a harmonic function from the surface deep into the object under study in order to obtain a temperature distribution function near sources is considered as a correction principle. This distribution is considered as an adjusted thermogram. The continuation is carried out on the basis of solving the Cauchy problem for the Laplace equation — an ill-posed problem. The solution is constructed using the Tikhonov regularization method. The main part of the constructed approximate solution is presented as a Fourier series by the eigenfunctions of the Laplace operator. Discretization of the problem leads to discrete Fourier series. A modification of the Hamming method for summing Fourier series and calculating their coefficients is proposed.

Key words and phrases: thermogram, ill-posed problem, Cauchy problem for the Laplace equation, Tikhonov regularization method, discrete Fourier series

1. Introduction

Thermal imaging methods are widely used in medicine as a means of early diagnostics [1–4]. Visualization (thermogram) of the temperature distribution on the surface of the patient's body contains information about sources of heat inside the body associated with the functioning of internal organs. In particular, it contains information about temperature anomalies associated with pathologies of internal organs. The image on the thermogram, as a rule,

© Laneev E. B., Baaj O., 2022



This work is licensed under a Creative Commons Attribution 4.0 International License

<https://creativecommons.org/licenses/by-nc/4.0/legalcode>

is distorted due to the process of thermal conductivity, heat exchange and the relative remoteness of heat sources from the surface of the body.

Within the framework of the chosen mathematical model, it is possible to correct the image on the thermogram in order to increase the effectiveness of diagnostics. Since the evolution of the temperature distribution in the patient's body is relatively slow, it makes it possible to use stationary models, in particular, models of harmonic temperature distribution. As an adjusted thermogram, we will consider the temperature distribution near the sources obtained by the continuation of the harmonic function from the boundary (similar to the continuation of gravitational fields in geophysics problems [5]).

In [6], based on the method [7], one of the possible solutions to such a problem is proposed. The problem, as ill-posed, is solved using the Tikhonov regularization method [8]. When forming computational algorithms, discrete Fourier series [9, 10] are used, the coefficients of which are calculated from functions depending on the coefficient number [11]. To sum up such series, a modification of the Hamming method [9] is proposed here.

2. Mathematical model and inverse problem

As a mathematical model, we consider a homogeneous heat-conducting body in the form of a rectangular cylinder

$$D(F, \infty) = \{(x, y, z) : 0 < x < l_x, 0 < y < l_y, F(x, y) < z < \infty\} \subset \mathbb{R}^3, \quad (1)$$

limited by the surface

$$S = \{(x, y, z) : 0 < x < l_x, 0 < y < l_y, z = F(x, y)\}. \quad (2)$$

We'll assume that we also know that

$$a_1 < F(x, y) < a_2 < H, \quad (x, y) \in \Pi, \quad (3)$$

$$\Pi = \{(x, y) : 0 < x < l_x, 0 < y < l_y\}. \quad (4)$$

The domain $D(F, \infty)$ contains heat sources with a time-independent density function ρ , creating a stationary (harmonic) temperature distribution in the body. We associate the density function of heat sources with the anomalies under study. We assume that on side faces Γ of the cylindrical domain $D(F, \infty)$ a temperature equal to zero is maintained, and on the surface S of the form (2) there is convective heat exchange with the external environment of temperature U_0 , described by Newton's law, according to which the density of the heat flux at the point of the surface S it is directly proportional to the temperature difference inside and outside.

It should be borne in mind from a physical point of view that despite the fact that the density of sources does not depend on time, the heat released by them is diverted across the boundary, the overall temperature distribution does not change over time, although the distribution gradient corresponds to stationary heat flows.

In the domain $D(F, \infty)$ of the form (1), the temperature distribution is the solution of a mixed boundary value problem for the Laplace equation

$$\begin{cases} \Delta u(M) = \rho(M), & M \in D(F, \infty), \\ \frac{\partial u}{\partial n} \Big|_S = h(U_0 - u) \Big|_S, \\ u|_{\Gamma} = 0, \\ u \text{ is bounded at } z \rightarrow \infty. \end{cases} \quad (5)$$

We assume that the function ρ is such that the solution of the problem (5) exists in $C^2(D(F, \infty)) \cap C^1(\overline{D(F, \infty)})$. In particular, the solution of the problem (5) allows us to find $u|_S$, i.e. the temperature distribution u on the surface of S , which we will call a thermogram.

Now let the thermogram be obtained as a result of measurements and the density of ρ is unknown. Let us now set the inverse problem. We set the problem of continuation of the temperature distribution from the surface towards the sources in order to obtain an adjusted thermogram as the temperature distribution $u|_{z=H}$ on the plane $z = H$, closer to the density carrier than the surface S . The plane $z = H$ is related to the surface S by the condition (3).

We assume that the carrier of the function ρ is located in the domain $z > H$, then the solution of the problem (5) in the domain

$$D(F, H) = \{(x, y, z) : 0 < x < l_x, 0 < y < l_y, F(x, y) < z < H\} \quad (6)$$

satisfies the Laplace equation. The set of side faces of the domain $D(F, H)$ is denoted by Γ_H .

Inverse problem. Let the function be given within the framework of the model (5)

$$f = u|_S, \quad (7)$$

and the density of ρ is unknown. It is required to find $u|_{z=H}$. It is required to find $u|_{z=H}$.

Since the value of H sufficiently arbitrarily defines the plane between the support of ρ and the surface S , then in fact the inverse problem consists in obtaining a solution u in the domain $D(F, H)$ (6) of the boundary value problem

$$\begin{cases} \Delta u(M) = 0, & M \in D(F, H), \\ u|_S = f, \\ \frac{\partial u}{\partial n} \Big|_S = h(U_0 - f) \Big|_S, \\ u|_{\Gamma_H} = 0. \end{cases} \quad (8)$$

We assume that the function f in (7), (8) is taken from the set of solutions to the direct problem (5), so the solution to the inverse problem exists in $C^2(D(F, H)) \cap C^1(\overline{D(F, H)})$.

Note that in the problem (8) on the surface S of the form (2), Cauchy conditions are set, that is, the boundary values f of the desired function u and the values of its normal derivative are set, so the problem (8) has a unique

solution. The boundary $z = H$ of the domain $D(F, H)$ is free and, thus, the problem (8) is unstable with respect to errors in the data, i.e. ill-posed.

The function $u|_{z=H}$ will be considered as an adjusted thermogram. Since the plane $z = H$ is located closer to the support of density ρ , it should be expected that the corrected thermogram more accurately conveys information about the distribution of heat sources than the original thermogram.

3. Approximate solution of the inverse problem.

Let the function f in the problem (8) be given with an error, that is, instead of f , the function f^δ is given, so that

$$\|f^\delta - f\|_{L_2(\Pi)} \leq \delta.$$

In [6], an approximate solution of the ill-posed problem (8) is constructed in the form

$$v_\alpha^\delta(M) = v_\alpha^\delta(M) + \Phi^\delta(M), \quad M \in D(F, H), \tag{9}$$

where function (integral over a rectangle Π of the form (4))

$$\begin{aligned} \Phi^\delta(M) = \int_{\Pi} & \left[h(U_0 - f^\delta(x_P, y_P))\varphi(M, P)|_{P \in S} n_1(x_P, y_P) - \right. \\ & \left. - f^\delta(x_P, y_P)(\mathbf{n}_1, \nabla_P \varphi(M, P))|_{P \in S} \right] dx_P dy_P \tag{10} \end{aligned}$$

is calculated using the problem (8) data, the Dirichlet problem source function

$$\begin{aligned} \varphi(M, P) = \frac{2}{l_x l_y} \sum_{n,m=1}^{\infty} \frac{e^{-k_{nm}|z_M - z_P|}}{k_{nm}} \times \\ \times \sin \frac{\pi n x_M}{l_x} \sin \frac{\pi m y_M}{l_y} \sin \frac{\pi n x_P}{l_x} \sin \frac{\pi m y_P}{l_y} \end{aligned}$$

in the cylinder

$$D^\infty = \{(x, y, z) : 0 < x < l_x, 0 < y < l_y, -\infty < z < \infty\} \subset \mathbb{R}^3,$$

the normal to the surface S of the form (2)

$$\mathbf{n}_1 = \text{grad}(F(x, y) - z) = \nabla_{xy} F - \mathbf{k}, \quad n_1 = |\mathbf{n}_1|.$$

The function v_α^δ , which is an approximation to the density potential ρ [12] was obtained in [6] using the Tikhonov regularization method [5]

$$v_\alpha^\delta(M) = - \sum_{n,m=1}^{\infty} \frac{\tilde{\Phi}_{nm}^\delta(a) \exp\{k_{nm}(z_M - a)\}}{1 + \alpha \exp\{2k_{nm}(H - a)\}} \sin \frac{\pi n x_M}{l_x} \sin \frac{\pi m y_M}{l_y}, \tag{11}$$

where $\alpha > 0$,

$$k_{nm} = \pi \left(\frac{n^2}{l_x^2} + \frac{m^2}{l_y^2} \right)^{1/2},$$

$\tilde{\Phi}_{nm}^\delta(a)$ — Fourier coefficients of the function $\Phi^\delta(M)$ of the form (10)

$$\tilde{\Phi}_{nm}^\delta(a) = \frac{4}{l_x l_y} \int_{\Pi} \Phi^\delta(x, y, a) \sin \frac{\pi n x}{l_x} \sin \frac{\pi m y}{l_y} dx dy, \quad a < a_1. \quad (12)$$

For the Fourier coefficients $\tilde{\Phi}_{nm}^\delta(a)$ in [11] the expression

$$\tilde{\Phi}_{nm}^\delta(a) = \tilde{\Phi}_{1,nm}^\delta(a) + \tilde{\Phi}_{2,nm}^\delta(a) \quad (13)$$

is obtained, where

$$\begin{aligned} \tilde{\Phi}_{1,nm}^\delta(a) = & \frac{4}{l_x l_y} \int_{\Pi} \left[h(U_0 - f^\delta(x, y)) \times \right. \\ & \left. \times \frac{e^{-k_{nm}(F(x,y)-a)}}{2k_{nm}} n_1(x, y) \sin \frac{\pi n x}{l_x} \sin \frac{\pi m y}{l_y} \right] dx dy, \quad (14) \end{aligned}$$

$$\begin{aligned} \tilde{\Phi}_{2,nm}^\delta(a) = & \\ = & \frac{4}{l_x l_y} \int_{\Pi} f^\delta(x, y) \frac{\pi n e^{-k_{nm}(F(x,y)-a)}}{2l_x k_{nm}} F'_x(x, y) \cos \frac{\pi n x}{l_x} \sin \frac{\pi m y}{l_y} dx dy + \\ + & \frac{4}{l_x l_y} \int_{\Pi} f^\delta(x, y) \frac{\pi m e^{-k_{nm}(F(x,y)-a)}}{2l_y k_{nm}} F'_y(x, y) \sin \frac{\pi n x}{l_x} \cos \frac{\pi m y}{l_y} dx dy + \\ + & \frac{2}{l_x l_y} \int_{\Pi} f^\delta(x, y) e^{-k_{nm}(F(x,y)-a)} \sin \frac{\pi n x}{l_x} \sin \frac{\pi m y}{l_y} dx dy. \quad (15) \end{aligned}$$

Thus, the Fourier coefficients $\tilde{\Phi}_{nm}^\delta(a)$ are calculated as the sum of formally calculated Fourier coefficients in accordance with (12) over orthogonal systems

$$\begin{aligned} \left\{ \sin \frac{\pi n x}{l_x} \sin \frac{\pi m y}{l_y} \right\}_{n,m=1}^{\infty}, \quad \left\{ \cos \frac{\pi n x}{l_x} \sin \frac{\pi m y}{l_y} \right\}_{n,m=1}^{\infty}, \\ \left\{ \sin \frac{\pi n x}{l_x} \cos \frac{\pi m y}{l_y} \right\}_{n,m=1}^{\infty}, \quad (16) \end{aligned}$$

of functions depending, apart from the arguments x and y , on the number nm of the Fourier coefficients.

4. Formation of an approximate solution based on discrete Fourier series

When discretizing the [13] problem (8) and performing numerical calculations using the formulas (11), (13), (14), (15) it is natural to pass to calculating the values of the approximate solution of the problem (8) on the grid of the values of the arguments x and y

$$\omega = \left\{ (x_i, y_j) : x_i = \frac{il_x}{N_x}, i = 0, 1, \dots, N_x, y_j = \frac{jl_y}{N_y}, j = 0, 1, \dots, N_y \right\}. \tag{17}$$

In this case, there is no need to use infinite Fourier series. One can pass to discrete Fourier series [9, 10], in this case two-dimensional.

The discrete Fourier series has an interpolation property, that is, the discrete Fourier series (by definition, representing a finite sum) with coefficients calculated by the corresponding formulas coincides on the grid with the values of the function. For example, if on the grid

$$x_i = i \frac{l}{N}, \quad i = 0, 1, \dots, N, \tag{18}$$

the grid function $f = (f_0, f_1, \dots, f_{N-1}, f_N)$ is given (when expanding into a discrete Fourier series in terms of sines, we assume that $f_0 = f_N = 0$). Then the function f can be represented by a discrete Fourier series in terms of sines [10]

$$f_i = \sum_{k=1}^{N-1} b_k \sin \frac{\pi k x_i}{l} = \sum_{k=1}^{N-1} b_k \sin \frac{\pi k i}{N}, \quad i = 0, 1, \dots, N, \tag{19}$$

where the coefficients b_k are calculated by the formula (equivalent to the trapezoid formula for the corresponding integral in the theory of Fourier series):

$$b_k = \frac{2}{N} \sum_{i=1}^{N-1} f_i \sin \frac{\pi k i}{N}, \quad k = 1, \dots, N - 1. \tag{20}$$

In other words, if the discrete series coefficients are calculated in accordance with the formula (20), then the discrete series (19) is exactly equal to the values of the function $f_i, i = 0, 1, \dots, N$.

Applying discrete Fourier series to the approximate solution (9) on the grid (17) for each fixed $z, a_2 < z < H$, will lead to the formula for v_α^δ :

$$(v_\alpha^\delta)_{ij}(z) = - \sum_{m=1}^{N_y-1} \sum_{n=1}^{N_x-1} \frac{\tilde{\Phi}_{nm}^\delta(a) \exp\{k_{nm}(z-a)\}}{1 + \alpha \exp\{2k_{nm}(H-a)\}} \sin \frac{\pi n i}{N_x} \sin \frac{\pi m j}{N_y}, \tag{21}$$

$$i = 0, \dots, N_x, \quad j = 0, \dots, N_y.$$

In this case, the integrals in calculating $\tilde{\Phi}_{nm}^\delta(a)$ by the formulas (13), (15), (14) it is natural to replace with formulas corresponding to the calculation of the coefficients of the discrete Fourier series of the form

$$\begin{aligned} \tilde{\Phi}_{nm}^\delta(a) = & \frac{4}{N_x N_y} \sum_{i=1}^{N_x-1} \sum_{j=1}^{N_y-1} f_{ij}(n, m) \sin \frac{\pi n i}{N_x} \sin \frac{\pi m j}{N_y} + \\ & + \frac{4}{N_x N_y} \sum_{i=1}^{N_x-1} \sum_{j=1}^{N_y-1} g_{ij}(n, m) \cos \frac{\pi n i}{N_x} \sin \frac{\pi m j}{N_y} + \\ & + \frac{4}{N_x N_y} \sum_{i=1}^{N_x-1} \sum_{j=1}^{N_y-1} p_{ij}(n, m) \sin \frac{\pi n i}{N_x} \cos \frac{\pi m j}{N_y}, \quad (22) \end{aligned}$$

($n = 1, 2, \dots, N_x - 1, m = 1, 2, \dots, N_y - 1$) on the grid ω of the form (17). To simplify the notation of integrands in integrals corresponding to systems (16), the notation f, g, p is introduced. A feature of calculating the coefficients of a discrete series in this case is that the functions f, g, p , in addition to the arguments x_i and y_j , depend on the indices n and m of the Fourier coefficients.

5. Summation of a discrete Fourier series and calculation of its coefficients by the Hamming method

Here we give some modification of the Hamming method [9] and its proof, related to the representation of a function as a discrete Fourier series in terms of sines or cosines on the interval $[0, l]$.

We now assume that the coefficients of the discrete series of some grid function w

$$w_i = \sum_{k=1}^{N-1} b_k \sin \frac{\pi k i}{N}, \quad i = 0, 1, \dots, N \quad (23)$$

are calculated formally in accordance with (20), where the values of the function f formally depend on the number k of the coefficient b_k , i.e.

$$b_k = \frac{2}{N} \sum_{i=1}^{N-1} f_i(k) \sin \frac{\pi k i}{N} = \frac{2}{N} \sum_{i=0}^N f_i(k) \sin \frac{\pi k i}{N}, \quad k = 1, \dots, N - 1 \quad (24)$$

while maintaining the condition

$$f_0(k) = f_N(k) = 0. \quad (25)$$

Let us show that the idea of Hamming algorithm [9] for calculating coefficients b_k of a discrete Fourier series (23) is also applicable to this situation, that is, to calculating the sum (24).

We fix the number k of the Fourier coefficient. Let us denote for brevity $t_k = \pi k/N$ and consider the recurrent formulas

$$\begin{cases} U_0 = 0, \\ U_1 = f_N(k), \\ U_m = (2 \cos t_k) U_{m-1} - U_{m-2} + f_{N-m+1}(k), \quad m = 2, 3, \dots, N. \end{cases} \quad (26)$$

Our task is to show that the Fourier coefficients b_k of the form (24) of the function w of the form (23) can be calculated by the formula

$$b_k = \frac{2}{N} \sum_{i=0}^N f_i(k) \sin \frac{\pi ki}{N} = \frac{2}{N} U_N \sin t_k, \tag{27}$$

where U_N is calculated by recurrent formulas (26).

For simplicity of notation, the dependence of U_m on k is not indicated. Note also that the recurrent formulas (26) use the values $f_N(k), \dots, f_1(k)$, the value $f_0(k)$ is not used when forming U_N .

Algorithm (26), (27) obviously allows to avoid calculation of sines in (24) with argument $\pi ki/N$ when changing indices i and k .

Let us represent the function $f(k)$ as a sum of functions $f^{(i)}(k)$, each of which is a vector with zero coordinates, except for the coordinate with number i equal to $f_i(k)$, that generally speaking, not equal to zero:

$$f(k) = \sum_{i=0}^N f^{(i)}(k), \tag{28}$$

$$f^{(i)}(k) = (f_0^{(i)}(k), \dots, f_N^{(i)}(k)) = (0, 0, \dots, 0, f_i(k), 0, \dots, 0).$$

Note that if the upper and lower indices do not coincide, the coordinate of the function $f^{(i)}(k)$ is equal to zero. Note also that when the grid function is represented by a sine series, due to (25) $f^{(0)}(k) = f^{(N)}(k) = (0, 0, \dots, 0)$.

We apply the recursive formulas (26) to each function $f^{(i)}(k)$, $i = 0, 1, 2, \dots, N$ (for a fixed k), denoting result as $U^{(i)}$:

$$\begin{cases} U_0^{(0)} = 0, \\ U_1^{(0)} = f_N^{(0)}(k), \\ U_m^{(0)} = 2 \cos t_k U_{m-1}^{(0)} - U_{m-2}^{(0)} + f_{N-m+1}^{(0)}(k), \quad m = 2, 3, \dots, N, \end{cases}$$

$$\begin{cases} U_0^{(1)} = 0, \\ U_1^{(1)} = f_N^{(1)}(k), \\ U_m^{(1)} = 2 \cos t_k U_{m-1}^{(1)} - U_{m-2}^{(1)} + f_{N-m+1}^{(1)}(k), \quad m = 2, 3, \dots, N, \end{cases}$$

...

$$\begin{cases} U_0^{(i)} = 0, \\ U_1^{(i)} = f_N^{(i)}(k), \\ U_m^{(i)} = 2 \cos t_k U_{m-1}^{(i)} - U_{m-2}^{(i)} + f_{N-m+1}^{(i)}(k), \quad m = 2, 3, \dots, N, \end{cases}$$

...

$$\begin{cases} U_0^{(N)} = 0, \\ U_1^{(N)} = f_N^{(N)}(k), \\ U_m^{(N)} = 2 \cos t_k U_{m-1}^{(N)} - U_{m-2}^{(N)} + f_{N-m+1}^{(N)}(k), \quad m = 2, 3, \dots, N. \end{cases}$$

Summing up the corresponding parts of all equalities, due to the linearity of the recursive formulas, we obtain

$$\begin{cases} \sum_{i=0}^N U_0^{(i)} = 0, \\ \sum_{i=0}^N U_1^{(i)} = \sum_{i=0}^N f_N^{(i)}(k), \\ \sum_{i=0}^N U_m^{(i)} = 2 \cos t_k \sum_{i=0}^N U_{m-1}^{(i)} - \sum_{i=0}^N U_{m-2}^{(i)} + \sum_{i=0}^N f_{N-m+1}^{(i)}(k), \quad m = 2, 3, \dots, N. \end{cases}$$

Considering (28) for the sum $f^{(i)}(k)$ and taking the notation

$$\sum_{i=0}^N U_m^{(i)} = U_m, \quad m = 0, \dots, N, \quad (29)$$

we obtain the recurrent formulas (26). Thus, to prove the formula (27), it suffices to calculate $U_N^{(i)}$ for all $i = 0, \dots, N$.

Let us calculate $U_N^{(i)}$, singling out the cases $i = 0, 1, N$ separately. Applying the recurrent formulas (26) to $f^{(i)}(k)$ for $i = 0, 1$ gives

$$\begin{cases} \begin{cases} U_0^{(0)} = 0, \\ U_1^{(0)} = f_N^{(0)}(k) = 0, \\ U_2^{(0)} = f_{N-1}^{(0)}(k) = 0, \\ \dots \\ U_{N-1}^{(0)} = f_2^{(0)}(k) = 0, \\ U_N^{(0)} = f_1^{(0)}(k) = 0 = V_0^{(0)}, \end{cases} & \begin{cases} U_0^{(1)} = 0, \\ U_1^{(1)} = f_N^{(1)}(k) = 0, \\ U_2^{(1)} = f_{N-1}^{(1)}(k) = 0, \\ \dots \\ U_{N-1}^{(1)} = f_2^{(1)}(k) = 0 = V_0^{(1)}, \\ U_N^{(1)} = f_1^{(1)}(k) = f_1(k) = V_1^{(1)}. \end{cases} \end{cases} \quad (30)$$

Applying the recurrent formulas (26) to $f^{(i)}(k)$ for $i = N$ gives

$$\begin{cases} U_0^{(N)} = 0 = V_0^{(N)}, \\ U_1^{(N)} = f_N^{(N)}(k) = f_N(k) = V_1^{(N)}, \\ \dots \\ U_m^{(N)} = (2 \cos t_k) V_{m-1}^{(N)} - V_{m-2}^{(N)}, \quad m = 2, 3, \dots, N. \end{cases} \quad (31)$$

Note that for all values of $m = 2, 3, \dots, N$ in (31) the value $f_{N-m+1}^{(N)}(k) = 0$, since the upper index is not equal to the lower one.

Applying the recurrent formulas (26) to $f^{(i)}(k)$ for $i = 2, \dots, N - 1$ gives

$$\begin{cases} U_0^{(i)} = 0, \\ \dots \\ U_{N-i}^{(i)} = f_{N-(N-i)+1}^{(i)}(k) = f_{i+1}^{(i)}(k) = 0 = V_0^{(i)}, \\ U_{N-i+1}^{(i)} = f_{N-(N-i+1)+1}^{(i)}(k) = f_i^{(i)}(k) = f_i(k) = V_1^{(i)}, \\ U_{N-i+m}^{(i)} = (2 \cos t_k)V_{m-1}^{(i)} - V_{m-2}^{(i)}, \quad m = 2, 3, \dots, i. \end{cases} \tag{32}$$

Here we took into account that $f_{N-(N-i+m)+1}^{(i)}(k) = f_{i+1-m}^{(i)}(k) = 0$, $m = 2, 3, \dots, i$, because the upper and lower indices do not match.

In the formulas (30), (31), (32) we introduced the notation

$$U_{N-i+m}^{(i)} = V_m^{(i)}, \quad i = 0, \dots, N, \quad m = 0, 1, 2, \dots, i. \tag{33}$$

It is easy to see that quantities $V_m^{(i)}$ are calculated using the same formulas (26), “skipping” the first $N - i - 1$ zeros for $U_m^{(i)}$. The introduction of the quantity $V_m^{(i)}$ allows us to obtain an explicit formula for it:

$$V_m^{(i)} = f_i(k) \frac{\sin mt_k}{\sin t_k}, \quad m = 0, 1, \dots, i, \tag{34}$$

for each $i = 0, 1, \dots, N$.

Let us prove it using the method of induction for m . As follows from (30), (32), this equality holds for $m = 0, 1$. Let’s prove it for $m = 0, 1, \dots, i$. Let equality (34) hold for $m - 2$ and $m - 1$. Let’s prove for m .

$$\begin{aligned} V_m^{(i)} &= (2 \cos t_k)V_{m-1}^{(i)} - V_{m-2}^{(i)} = \\ &= f_i(k) \left[2 \cos t_k \frac{\sin(m-1)t_k}{\sin t_k} - \frac{\sin(m-2)t_k}{\sin t_k} \right] = \\ &= f_i(k) \left[\frac{\sin mt_k + \sin(m-2)t_k - \sin(m-2)t_k}{\sin t_k} \right] = f_i(k) \frac{\sin mt_k}{\sin t_k}. \end{aligned}$$

Note that from (33), in particular, $U_N^{(i)} = V_i^{(i)}$ and from the formula (34) for $m = i$ we obtain

$$U_N^{(i)} = V_i^{(i)} = f_i(k) \frac{\sin it_k}{\sin t_k}. \tag{35}$$

Summing according to (29) with $m = N$, and using (24), we obtain

$$U_N = \sum_{i=0}^N U_N^{(i)} = \sum_{i=0}^N V_i^{(i)} = \frac{1}{\sin t_k} \sum_{i=0}^N f_i(k) \sin it_k = b_k \frac{1}{\sin t_k} \frac{N}{2}.$$

From here we obtain the formula (27).

Let us now proceed to calculating the coefficients of the discrete Fourier series of the grid function w in cosine expansion. On the same grid (18) consider the discrete Fourier series in cosines expansion [10]

$$w_i = \frac{a_0}{2} + \sum_{k=1}^{N-1} a_k \cos \frac{\pi k i}{N} + \frac{a_N}{2} (-1)^i, \quad i = 0, 1, \dots, N, \quad (36)$$

whose coefficients a_k are calculated on the basis of the grid function f depending on the number k by the formula

$$a_k = \frac{2}{N} \left(\frac{f_0(k)}{2} + \sum_{i=1}^{N-1} f_i(k) \cos \frac{\pi k i}{N} + \frac{f_N(k)}{2} (-1)^k \right). \quad (37)$$

We introduce the grid function

$$\tilde{f}(k) = \left(\frac{f_0(k)}{2}, f_1(k), f_2(k), \dots, f_{N-1}(k), \frac{f_N(k)}{2} \right), \quad (38)$$

that differs from f in that the current and last coordinates are divided in half. Replacing f in (26) with \tilde{f} , we get formulas (33), (34).

Note that the recurrent formulas (30) for $i = 0$ imply $U_N^{(0)} = 0$, $U_{N-1}^{(0)} = 0$. For $i = 1, 2, \dots, N$ from (33), (34) we obtain

$$U_{N-1}^{(i)} = V_{i-1}^{(i)} = \tilde{f}_i(k) \frac{\sin(i-1)t_k}{\sin t_k}, \quad i = 1, 2, \dots, N. \quad (39)$$

Consider the following construction (summation starts from $i = 1$, since $U_N^{(0)} = U_{N-1}^{(0)} = 0$):

$$\begin{aligned} \cos t_k U_N - U_{N-1} + \tilde{f}_0(k) &= \cos t_k \sum_{i=1}^N U_N^{(i)} - \sum_{i=1}^N U_{N-1}^{(i)} + \tilde{f}_0(k) = \\ &= \sum_{i=1}^N [\cos t_k U_N^{(i)} - U_{N-1}^{(i)}] + \tilde{f}_0(k). \end{aligned}$$

Replacing $U_N^{(i)}$ and $U_{N-1}^{(i)}$ according to formulas (35) and (39), we obtain

$$\begin{aligned} \cos t_k U_N - U_{N-1} + \tilde{f}_0(k) &= \sum_{i=1}^N [\cos t_k V_i^{(i)} - V_{i-1}^{(i)}] + \tilde{f}_0(k) = \\ &= \sum_{i=1}^N \tilde{f}_i(k) \frac{\cos t_k \sin i t_k - \sin(i-1)t_k}{\sin t_k} + \tilde{f}_0(k) = \\ &= \sum_{i=1}^N \tilde{f}_i(k) \frac{\cos t_k \sin i t_k - \cos t_k \sin i t_k + \sin t_k \cos i t_k}{\sin t_k} + \tilde{f}_0(k) = \end{aligned}$$

$$\begin{aligned}
 &= \sum_{i=1}^N \tilde{f}_i(k) \cos it_k + \tilde{f}_0(k) = \tilde{f}_0(k) + \sum_{i=1}^{N-1} \tilde{f}_i(k) \cos it_k + \tilde{f}_N(k) \cos Nt_k = \\
 &= \frac{f_0(k)}{2} + \sum_{i=1}^{N-1} f_i(k) \cos it_k + \frac{f_N(k)}{2} (-1)^k.
 \end{aligned}$$

From here according to (37) we obtain a formula for the coefficients of the discrete Fourier series in the cosine expansion

$$a_k = \frac{2}{N} \left[\cos t_k U_N - U_{N-1} + \tilde{f}_0(k) \right] = \frac{2}{N} \left[\cos t_k U_N - U_{N-1} + \frac{f_0(k)}{2} \right], \quad (40)$$

moreover, the quantities U_N and U_{N-1} are calculated by the formulas (26), in which the grid function f is replaced by \tilde{f} , which is related to f by the formula (38).

Note that the formulas (26), (27) can also be used to sum the Fourier series (23), since the formulas (24) and (23) differ only by a factor. Note that when summing the series (23), we, of course, do not obtain $f(k)$, but we obtain some function w . Accordingly, the formulas (26), (40) can also be used to sum the Fourier series (36), since the formulas (37) and (36) differ only by the multiplier.

The formulas (26), (27), (40) can be used for two-dimensional discrete Fourier series both for calculating the coefficients and for summing the Fourier series (21). In this case, the formulas (26), (27) for each fixed pair nm are applied sequentially over each index i and j corresponding to the variables x and y .

The formulas (26), (40) for calculating the coefficients of the discrete Fourier series in cosine expansion, of course, are also valid in the case when $f_0 = f_N = 0$, which corresponds to the formulas (22).

6. Conclusion and discussion

Formulas (21), (22), (26), (27), (40) as a solution to the problem (8) can be used for mathematical processing of thermograms taken with a thermal imager in medicine [4] in order to correct the image on the thermogram. Note that taking into account the influence of blood flow leads to the need to use the metaharmonic equation [14], [15] in problem (8).

The thermogram, with one or another certainty, conveys an image of the structure of heat sources inside the body. However, within the framework of the task (8), the image on the thermogram can be refined. In this case, we consider the function f^δ as the original thermogram, and the function $v_\alpha^\delta|_{z=H}$ as the corrected thermogram. Since the function $v_\alpha^\delta|_{z=H}$ is the temperature distribution on a plane closer to the investigated heat sources than the original surface S , we can expect a more accurate reproduction of the source image on the calculated thermogram $v_\alpha^\delta|_{z=H}$.

The results of calculations performed on a model example show the effectiveness of the proposed method and algorithm based on the formulas (9), (10), (11), (13) that can be used for processing thermal images.

Note that the method of summation of discrete Fourier series, described in Section 5, can be used to solve other problems, the solutions of which can be obtained in the form of Fourier series in terms of eigenfunctions of the Laplace operator in a rectangle.

Acknowledgments

The research is supported by the Russian Foundation for Basic Research (grant №20-01-00610a).

References

- [1] E. F. J. Ring, “Progress in the measurement of human body temperature,” *IEEE Engineering in Medicine and Biology Magazine*, vol. 17, no. 4, pp. 19–24, 1998. DOI: 10.1109/51.687959.
- [2] E. Y. K. Ng and N. M. Sudarshan, “Numerical computation as a tool to aid thermographic interpretation,” *Journal of Medical Engineering and Technology*, vol. 25, no. 2, pp. 53–60, 2001. DOI: 10.1080/03091900110043621.
- [3] B. F. Jones and P. Plassmann, “Digital infrared thermal imaging of human skin,” *IEEE Eng. in Med. Biol. Mag.*, vol. 21, no. 6, pp. 41–48, 2002. DOI: 10.1109/memb.2002.1175137.
- [4] G. R. Ivanitskii, “Thermovision in medicine [Teplovideniye v meditsine],” *Vestnik RAN*, vol. 76, no. 1, pp. 44–53, 2006, in Russian.
- [5] A. N. Tikhonov, V. B. Glasko, O. K. Litvinenko, and V. R. Melihov, “On the continuation of the potential towards disturbing masses based on the regularization method [O prodolzhenii potentsiala v storonu vozmushchayushchih mass na osnove metoda regulyaryzatsii],” *Izvestiya AN SSSR. Fizika Zemli*, no. 1, pp. 30–48, 1968, in Russian.
- [6] E. B. Laneev, N. Y. Chernikova, and O. Baaj, “Application of the minimum principle of a Tikhonov smoothing functional in the problem of processing thermographic data,” *Advances in Systems Science and Applications*, vol. 1, pp. 139–149, 2021. DOI: 10.25728/assa.2021.21.1.1055.
- [7] E. B. Laneev, “Construction of a Carleman function based on the Tikhonov regularization method in an ill-posed problem for the Laplace equation,” *Differential Equations*, vol. 54, no. 4, pp. 476–485, 2018. DOI: 10.1134/S0012266118040055.
- [8] A. N. Tikhonov and V. J. Arsenin, *Methods for solving ill-posed problems [Metody resheniya nekorrektnykh zadach]*. Moscow: Nauka, 1979, in Russian.
- [9] R. W. Hamming, *Numerical methods for scientists and engineers*. New York: McGraw-Hill Book Company, 1962.
- [10] E. B. Laneev, *Numerical methods [Chislennyye metody]*. Moscow: RUDN, 2005, in Russian.

- [11] O. Baaj, "On the application of the Fourier method to solve the problem of correction of thermographic images," *Discrete and Continuous Models and Applied Computational Science*, vol. 30, no. 3, pp. 205–216, 2022. DOI: 10.22363/2658-4670-2022-30-3-205-216.
- [12] E. B. Laneev, *Ill-posed problems of continuation of harmonic functions and potential fields and methods for their solution [Nekorrektnye zadachi prodolzheniya garmonicheskikh funkciy i potencialnyh polej i metody ih resheniya]*. Moscow: RUDN, 2006, in Russian.
- [13] E. B. Laneev, M. N. Mouratov, and E. P. Zhidkov, "Discretization and its proof for numerical solution of a Cauchy problem for Laplace equation with inaccurately given Cauchy conditions on an inaccurately defined arbitrary surface," *Physics of Particles and Nuclei Letters*, vol. 5, no. 3, pp. 164–167, 2002. DOI: 10.1134/S1547477108030059.
- [14] H. Pennes, "Analysis of tissue and arterial blood temperature in the resting human forearm," *J. Appl. Physiol.*, no. 1, pp. 93–122, 1948.
- [15] J. P. Agnelli, A. A. Barrea, and C. V. Turner, "Tumor location and parameter estimation by thermography," *Mathematical and Computer Modelling*, vol. 53, no. 7–8, pp. 1527–1534, 2011. DOI: 10.1016/j.mcm.2010.04.003.

For citation:

E. B. Laneev, O. Baaj, On a modification of the Hamming method for summing discrete Fourier series and its application to solve the problem of correction of thermographic images, *Discrete and Continuous Models and Applied Computational Science* 30 (4) (2022) 342–356. DOI: 10.22363/2658-4670-2022-30-4-342-356.

Information about the authors:

Laneev, Evgeniy B. — Doctor of Physical and Mathematical Sciences, Professor of Mathematical Department of Peoples' Friendship University of Russia (RUDN University) (e-mail: elaneev@yandex.ru, phone: +7(903)1333622, ORCID: <https://orcid.org/0000-0002-4255-9393>, ResearcherID: G-7887-2016, Scopus Author ID: 24366681900)

Baaj, Obaida — Post-Graduate Student of Mathematical Department of Peoples' Friendship University of Russia (RUDN University) (e-mail: 1042175025@rudn.ru, phone: +7(916)6890863, ORCID: <https://orcid.org/0000-0003-4813-7981>, ResearcherID: ADK-3603-2022, Scopus Author ID: 57222870471)

УДК 519.6

PACS 07.05.Tr, 02.60.Pn, 02.70.Bf

DOI: 10.22363/2658-4670-2022-30-4-342-356

Об одной модификации метода Хемминга суммирования дискретных рядов Фурье и её применение для решения задачи коррекции термографических изображений

Е. Б. Ланеев, Обаида Бааж

*Российский университет дружбы народов,
ул. Миклуто-Маклая, д. 6, Москва, 117198, Россия*

Аннотация. В работе рассматриваются математические методы коррекции термографических изображений (термограмм), полученных с помощью тепловизора, в виде распределения температуры на поверхности исследуемого объекта. Термограмма воспроизводит изображение тепловыделяющих структур, расположенных внутри исследуемого объекта. Это изображение передаётся с искажениями, так как источники, как правило, удалены от его поверхности и распределение температуры на поверхности объекта передаёт изображение как размытое за счёт процессов теплопроводности и теплопереноса. В работе в качестве принципа коррекции рассматривается продолжение функции температуры как гармонической функции с поверхности вглубь исследуемого объекта с целью получения функции распределения температуры вблизи источников. Такое распределение рассматривается как скорректированная термограмма. Продолжение функции температуры осуществляется на основе решения задачи Коши для уравнения Лапласа — некорректно поставленной задачи. Построение решения проводится с использованием метода регуляризации Тихонова. Основная часть построенного приближённого решения представлена в виде ряда Фурье по собственным функциям оператора Лапласа. Дискретизация задачи приводит к дискретным рядам Фурье. Для суммирования рядов Фурье и вычисления коэффициентов в работе предложена модификация метода Хемминга.

Ключевые слова: термограмма, некорректная задача, задача Коши для уравнения Лапласа, метод регуляризации Тихонова, дискретный ряд Фурье



UDC 519.872:519.217

PACS 07.05.Tp, 02.60.Pn, 02.70.Bf

DOI: 10.22363/2658-4670-2022-30-4-357-363

Profile thickness synthesis of thin-film waveguide Luneburg lens

Konstantin P. Lovetskiy¹,
Anton L. Sevastianov², Alexander V. Zorin¹

¹ Peoples' Friendship University of Russia (RUDN University),
6, Miklukho-Maklaya St., Moscow, 117198, Russian Federation

² Higher School of Economics (HSE University),
11, Pokrovsky Bulvar, Moscow, 109028, Russian Federation

(received: November 1, 2022; revised: December 12, 2022; accepted: December 19, 2022)

Abstract. In the work the link between the focusing inhomogeneity of the effective refractive index of waveguide Luneburg lens and the irregularity of the waveguide layer thickness generating this inhomogeneity is demonstrated. For the dispersion relation of irregular thin-film waveguide in the model of adiabatic waveguide modes the problem of mathematical synthesis and computer-aided design of the waveguide layer thickness profile for the Luneburg thin-film generalized waveguide lens with a given focal length is being solved. The calculations are carried out in normalized (in a special way) coordinates to adapt the used relations to computer calculations. The obtained solution is compared with the same solution within the cross-section's method. The performance of the algorithm implemented in Delphi, was demonstrated by plotting the dispersion curves and plotting a family of dispersion curves, demonstrating a critical convergence. As an additional result, the thickness profiles of additional (irregular in thickness) waveguide layer, forming a thin film generalized waveguide Luneburg lens were synthesized. This result generalizes Southwell's results.

Key words and phrases: Luneburg waveguide lens, effective refractive index inhomogeneity, section method, waveguide adiabatic mode model

1. Model of adiabatic waveguide modes

Using the example of a thin film generalized waveguide Luneburg (TGWL) lens (see figure 1), which performs a two-dimensional Fourier transform with a finite aperture, the application of the adiabatic mode model is demonstrated. The inverse problem of synthesizing a thin film generalized waveguide Luneburg (TGWL) lens is solved within the framework of the model of adiabatic waveguide modes.

© Lovetskiy K. P., Sevastianov A. L., Zorin A. V., 2022



This work is licensed under a Creative Commons Attribution 4.0 International License

<https://creativecommons.org/licenses/by-nc/4.0/legalcode>

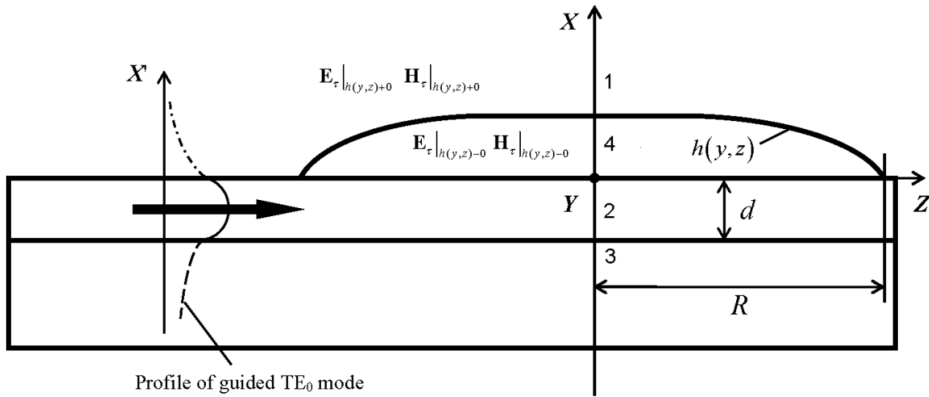


Figure 1. Cross section of the TGWL under consideration

Solutions of the Maxwell’s equations for adiabatic waveguide modes are sought in the form [1]:

$$\begin{Bmatrix} \mathbf{E}(x, y, z, t) \\ \mathbf{H}(x, y, z, t) \end{Bmatrix} = \begin{Bmatrix} \tilde{\mathbf{E}}(x, y, z, t) \\ \tilde{\mathbf{H}}(x, y, z, t) \end{Bmatrix} \frac{\exp\{i\omega t - i\varphi(y, z)\}}{\sqrt{\beta(y, z)}},$$

where

$$\beta_y(y, z) = \frac{1}{k_0} \left(\frac{\partial \varphi}{\partial y} \right), \quad \beta_z(y, z) = \frac{1}{k_0} \left(\frac{\partial \varphi}{\partial z} \right),$$

$$\beta(y, z) = \sqrt{\beta_y(y, z)^2 + \beta_z(y, z)^2}.$$

In a multilayer waveguide, in the zeroth approximation, the equations for the leading components of the electromagnetic field of adiabatic waveguide modes take the form [2–5]:

$$\frac{d^2 \tilde{E}_z^0}{d\tilde{x}^2} + (\tilde{\varepsilon} \tilde{\mu} - \tilde{\beta}^2) \tilde{E}_z^0 = 0, \quad \frac{d^2 \tilde{H}_z^0}{d\tilde{x}^2} + (\tilde{\varepsilon} \tilde{\mu} - \tilde{\beta}^2) \tilde{H}_z^0 = 0.$$

The expressions for the remaining four components of the electromagnetic field take the form:

$$\tilde{H}_x^0 = \frac{1}{\tilde{\varepsilon} \tilde{\mu} - \tilde{\beta}_z^2} \left[-i \tilde{\beta}_z \frac{d \tilde{H}_z^0}{d\tilde{x}} + \tilde{\varepsilon} \tilde{\beta}_y \tilde{E}_z^0 \right], \quad \tilde{H}_y^0 = \frac{1}{\tilde{\varepsilon} \tilde{\mu} - \tilde{\beta}_z^2} \left[-i \tilde{\varepsilon} \frac{d \tilde{E}_z^0}{d\tilde{x}} - \tilde{\beta}_z \tilde{\beta}_y \tilde{H}_z^0 \right],$$

$$\tilde{E}_x^0 = \frac{1}{\tilde{\varepsilon} \tilde{\mu} - \tilde{\beta}_z^2} \left[-i \tilde{\beta}_z \frac{d \tilde{E}_z^0}{d\tilde{x}} - \tilde{\mu} \tilde{\beta}_y \tilde{H}_z^0 \right], \quad \tilde{E}_y^0 = \frac{1}{\tilde{\varepsilon} \tilde{\mu} - \tilde{\beta}_z^2} \left[i \tilde{\mu} \frac{d \tilde{H}_z^0}{d\tilde{x}} - \tilde{\beta}_z \tilde{\beta}_y \tilde{E}_z^0 \right].$$

In subdomains (waveguide layers) with constant refractive indices $n_j^2 = \varepsilon_j \mu_j$, solutions from the fundamental system of solutions are written as linear combinations of exponentials. Substituting them all into the boundary equations,

after reducing similar terms, we obtain homogeneous linear equations for indefinite amplitude coefficients $\tilde{A}_s, \tilde{B}_s, \tilde{A}_f^\pm, \tilde{B}_f^\pm, \tilde{A}_l^\pm, \tilde{B}_l^\pm, \tilde{A}_c, \tilde{B}_c$. This system with a matrix admits non-trivial solutions under the condition [1]:

$$\det M(\beta(r)) = 0.$$

The solution of given nonlinear PDE of the first order with respect to $h(r)$ synthesizes the proper profile of Luneburg TGWL.

2. Mathematical synthesis of a thin film generalized waveguide Luneburg lens

In the works of Southwell [6, 7] the thickness profile of Luneburg TGWL with parameters $n_s = 1.47, n_f = 1.565, n_l = 2.10, n_c = 1.0, d = 1.0665\mu, \lambda = 0.5\mu$ was synthesized by the cross-section method in which precise boundary conditions for the Maxwell's equations are replaced by their approximations — projections on the horizontal plane [1]. The supporter of irregularity region of TGWL in the method of comparison waveguides automatically coincides with the supporter of $n_{\text{eff}}^j(r) = \beta_j(r)/\beta_j$ inhomogeneity of the two-dimensional TGWL of Luneburg: $\text{supp } h = \text{supp } n = \text{supp } \beta$.

The method of adiabatic waveguide modes does not require the matching of these two supporters. However, the fact that the irregularity of TGWL forces to focus a family of curves locally orthogonal to the focused wave front of the waveguide mode, that the region of waveguide irregularity does not exceed the circle $Q(F)$ of the radius F : $\text{supp } h \subseteq Q(F)$. Following this reasoning, we seek the thickness profile of the irregular waveguide layer $h(r)$ in a circle of radius F .

The equation [1] of the synthesis of the thickness profile of the irregular waveguide layer of Luneburg TGWL depends on the trajectories of the rays (parallel at the entrance to the irregularity region) and on their velocities derived from the equations for the rays that pass through the region of inhomogeneity. From ODE systems for $(y, z)^T(s)$ rays' equations

$$\frac{d}{ds} \left(\beta(y, z) \frac{dy}{ds} \right) = \frac{\partial \beta}{\partial y}(y, z), \quad \frac{d}{ds} \left(\beta(y, z) \frac{dz}{ds} \right) = \frac{\partial \beta}{\partial z}(y, s)$$

using substitution $\frac{dy}{dz} = V, A = \frac{1}{\beta} \frac{\partial \beta}{\partial z}, B = \frac{1}{\beta} \frac{\partial \beta}{\partial y}$, we obtain the equivalent system of ODEs other realization:

$$\frac{dy}{ds} = V, \quad \frac{dV}{dz} = (1 + V^2)(B - AV). \tag{1}$$

The Cauchy problem for the system (1) with the initial conditions

$$y(z_0) = y_0, \quad V(z_0) = 0, \tag{2}$$

we solve by the Runge–Kutta–Fehlberg method of the 6th order with automatically step selection [8] resulting in the family of “data” $y_j^F(z_k^j)$, $V_j^F(z_k^j)$ at the family of points, automatically generated while solving the problem (1), (2) for any beforehand defined focal distance F .

Data from the files $y_j^F(z_k^j)$, $V_j^F(z_k^j)$ allow calculating the components of the vector field of the phase delay $\vec{\beta} = (\beta_z, \beta_y)^T$ of AWM, for which $\beta(y, z) = \sqrt{\beta_y^2 + \beta_z^2}$ according to the formulas

$$\beta_y(z_k^j) = \frac{\beta(z_k^j)V(z_k^j)}{(1 + V^2(z_k^j))^{1/2}}, \quad \beta_z(z_k^j) = \frac{\beta(z_k^j)}{(1 + V^2(z_k^j))^{1/2}}. \quad (3)$$

The result of the calculations allows to complement the previously generated data file to $y_j^F(z_k^j)$, $V_j^F(z_k^j)$, $\beta_y^F(z_k^j)$, $\beta_z^F(z_k^j)$. Now we have at our disposal all the necessary data for the formulation of the problem of mathematical synthesis $h^F(r)$. The matrix $M(\beta^F)$ depends on the following variables

$$M(\beta^F) = M \left(n_s, n_f, n_l, n_c, d; \{z_k^j, y_k^j, V_k^j\}; \beta^F(y_k^j, z_k^j), \gamma_s^F(y_k^j, z_k^j), \gamma_c^F(y_k^j, z_k^j), \chi_f^F(y_k^j, z_k^j), \chi_l^F(y_k^j, z_k^j), \beta_y^F(y_k^j, z_k^j), \beta_z^F(y_k^j, z_k^j); h^F(z_k^j, y_k^j), \frac{\partial h^F}{\partial y}(z_k^j, y_k^j), \frac{\partial h^F}{\partial z}(z_k^j, y_k^j), F \right). \quad (4)$$

For the matrix $M(*; z_k^j, y_k^j; \dots, F)$ at each point of «phase-ray mesh» $\{z_k^j, y_k^j\}^F$ the condition $\det M(*; z_k^j, y_k^j; \dots, F) = 0$ must be fulfilled.

The approximation $h_N^F(r)$ of the function $h^F(r)$, which defines the thickness profile of the irregular waveguide layer, are sought in the form:

$$h_N^F(z, y) = \sum_{i=1}^N K_i \exp \left\{ -\frac{(y - y_c)^2 + (z - z_c)^2}{C_i^2} \right\}, \quad (5)$$

which allows calculating the explicit form of derivatives (see figure 2).

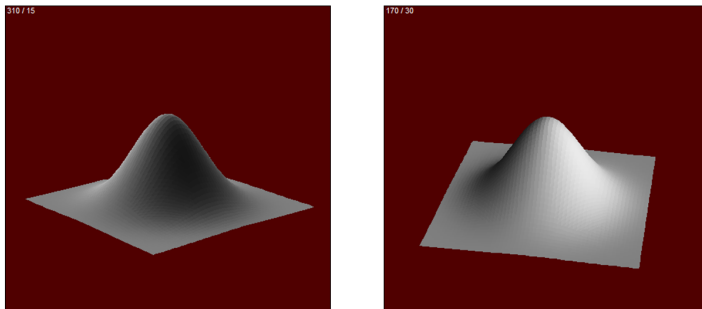


Figure 2. Plot of the approximate solution $h_N^F(z, y)$ of the thickness profile of the irregular waveguide layer of Luneburg TGWL

The search for the unknown coefficients (K_i, C_i) to construct an approximate solution $h^F(r)$ in (5) carried out by minimizing the objective function

$$F_{arg}(K_i, C_i) = \sum_{z_k^j, y_k^j} \left| \det M \left(h_N^F(z, y), \frac{\partial h_N^F(z, y)}{\partial y}, \frac{\partial h_N^F(z, y)}{\partial z} \right) \right|^2, \quad (6)$$

by the Nelder–Mead method [9, 10].

3. Conclusion

The paper discusses the problems of numerical implementation of the cross-section method to calculate an evolution of the mode in a smooth transition from one planar regular open waveguide to another. In the class of multi-layer thin-film dielectric waveguides the problem on eigenvalues and eigen guided modes can be reduced (by expansion in the fundamental system of solutions in separate layers) to solving a system of linear algebraic equations for the coefficients of expansion in the fundamental system of solutions. The condition of non-triviality of the resulting solution in this case is the condition for the vanishing of the determinant of the corresponding system of linear algebraic equations.

The paper describes the classical and generalized Luneburg lens in bulk and waveguide implementation. Then the link between the focusing inhomogeneity of the effective refractive index of waveguide Luneburg lens and the irregularity of the waveguide layer thickness generating this inhomogeneity demonstrated. For the dispersion relation of irregular thin-film waveguide in the model of AWM the problem of mathematical synthesis and computer-aided design of the waveguide layer thickness profile for Luneburg TGWL with a given focal length is being solved.

References

- [1] A. L. Sevastyanov, “Computer modeling of directed modes’ fields of thin-film generalized waveguide Luneburg lens. Candidate’s Dissertation in Physics and Mathematics [Komp’yuternoe modelirovanie polej napravlyaemyh mod tonkoplennoj obobshchennoj volnovodnoj linzy Lyuneberga],” in Russian, Ph.D. dissertation, Peoples’ Friendship University of Russia, Moscow, 2010.
- [2] L. A. Sevast’yanov and A. A. Egorov, “Theoretical analysis of the waveguide propagation of electromagnetic waves in dielectric smoothly-irregular integrated structures,” *Optics and Spectroscopy*, no. 105, pp. 576–584, 2008. DOI: 10.1134/S0030400X08100123.
- [3] A. A. Egorov and L. A. Sevast’yanov, “Structure of modes of a smoothly irregular integrated-optical four-layer three-dimensional waveguide,” *Quantum Electronics*, vol. 39, no. 6, pp. 566–574, 2009. DOI: 10.1070/QE2009v039n06ABEH013966.

- [4] A. A. Egorov, K. P. Lovetskii, A. L. Sevast'yanov, and L. A. Sevast'yanov, "Simulation of guided modes (eigenmodes) and synthesis of a thin-film generalised waveguide Luneburg lens in the zero-order vector approximation," *Quantum Electronics*, vol. 40, no. 9, pp. 830–836, 2010. DOI: 10.1070/QE2010v040n09ABEH014332.
- [5] L. A. Sevastianov, A. A. Egorov, and A. L. Sevastyanov, "Method of adiabatic modes in studying problems of smoothly irregular open waveguide structures," *Physics of Atomic Nuclei*, vol. 76, pp. 224–239, 2013. DOI: 10.1134/S1063778813010134.
- [6] W. H. Southwell, "Inhomogeneous optical waveguide lens analysis," *Journal of the Optical Society of America*, vol. 67, no. 8, pp. 1004–1009, 1977. DOI: 10.1364/JOSA.67.001004.
- [7] W. H. Southwell, "Index profiles for generalized Luneburg lenses and their use in planar optical waveguides," *Journal of the Optical Society of America*, vol. 67, no. 8, pp. 1010–1014, 1977. DOI: 10.1364/JOSA.67.001010.
- [8] E. Fehlberg, "Low-order Classical Runge-Kutta formulas with step size control," NASA Technical Report R-315, Tech. Rep., 1969.
- [9] A. L. Sevastyanov, "Structure of modes of smoothly irregular three-dimensional integrated optical four-layer waveguide," *Physics of Particles and Nuclei Letters*, vol. 8, no. 479, pp. 804–811, 2011. DOI: 10.1134/S1547477111050177.
- [10] A. A. Egorov *et al.*, "Stable computer modeling of thin-film generalized waveguide Luneburg lens [Ustojchivoe komp'yuternoe modelirovanie tonkoplenochnoj obobshchennoj volnovodnoj linzy Lyuneberga]," *Matem. modelirovaniye*, vol. 26, no. 11, pp. 37–44, 2014, in Russian.

For citation:

K. P. Lovetskiy, A. L. Sevastianov, A. V. Zorin, Profile thickness synthesis of thin-film waveguide Luneburg lens, *Discrete and Continuous Models and Applied Computational Science* 30 (4) (2022) 357–363. DOI: 10.22363/2658-4670-2022-30-4-357-363.

Information about the authors:

Lovetskiy, Konstantin P. — Candidate of Physical and Mathematical Sciences, Associate Professor of Department of Applied Probability and Informatics of Peoples' Friendship University of Russia (RUDN University) (e-mail: lovetskiy-kp@rudn.ru, phone: +7(495)9522572, ORCID: <https://orcid.org/0000-0002-3645-1060>)

Sevastianov, Anton L. — Candidate of Physical and Mathematical Sciences, Deputy Head of Department of Education digitalization of Higher School of Economics (HSE University) (e-mail: alsevastyanov@gmail.com, ORCID: <https://orcid.org/0000-0002-0280-485X>)

Zorin, Alexander V. — Doctor of Physical and Mathematical Sciences, Assistant Professor of Department of Applied Probability and Informatics of Peoples' Friendship University of Russia (RUDN University) (e-mail: zorin-av@rudn.ru, ORCID: <https://orcid.org/0000-0002-5721-4558>)

УДК 519.872:519.217

PACS 07.05.Tr, 02.60.Pn, 02.70.Bf

DOI: 10.22363/2658-4670-2022-30-4-357-363

Синтез толщины профиля тонкоплёночной волноводной линзы Люнеберга

К. П. Ловецкий¹, А. Л. Севастьянов², А. В. Зорин¹

¹ *Российский университет дружбы народов,
ул. Миклухо-Маклая, д. 6, Москва, 117198, Россия*

² *Высшая школа экономики,
Покровский бульвар, д. 11, Москва, 109028, Россия*

Аннотация. В работе показана связь между фокусирующей неоднородностью эффективного показателя преломления волноводной линзы Люнеберга и неравномерностью толщины волноводного слоя, порождающей эту неоднородность. Для закона дисперсии нерегулярного тонкоплёночного волновода в модели адиабатических мод волновода решается задача математического синтеза и компьютерного проектирования профиля толщины волноводного слоя для тонкоплёночной обобщённой волноводной линзы Люнеберга с заданным фокусным расстоянием. Расчёты ведутся в нормированных специальным образом координатах для адаптации используемых соотношений к компьютерным расчётам. Полученное решение сравнивается с таким же решением в рамках метода сечений. Работоспособность алгоритма, реализованного в Delphi, была продемонстрирована путём построения дисперсионных кривых и семейства дисперсионных кривых, показывающих критическую сходимость. В качестве дополнительного результата были синтезированы профили толщины дополнительного нерегулярного по толщине волноводного слоя, образующего тонкоплёночную обобщённую волноводную линзу Люнеберга. Этот результат обобщает результаты Саутвелла.

Ключевые слова: волноводная линза Люнеберга, неоднородность эффективного показателя преломления, метод сечений, модель адиабатических мод волновода



UDC 519.872:519.217

PACS 07.05.Tp, 02.60.Pn, 02.70.Bf

DOI: 10.22363/2658-4670-2022-30-4-364-373

Conservative finite difference schemes for dynamical systems

Yu Ying, Zhen Lu

*Kaili University,
Kaiyuan Road 3, Kaili, 556011, China*

(received: November 6, 2022; revised: December 8, 2022; accepted: December 19, 2022)

Abstract. The article presents the implementation of one of the approaches to the integration of dynamical systems, which preserves algebraic integrals in the original fdm for Sage system. This approach, which goes back to the paper by del Buono and Mastroserio, makes it possible, based on any two explicit difference schemes, including any two explicit Runge–Kutta schemes, to construct a new numerical algorithm for integrating a dynamical system that preserves the given integral. This approach has been implemented and tested in the original fdm for Sage system. Details and implementation difficulties are discussed. For testing, two Runge–Kutta schemes were taken having the same order, but different Butcher tables, which does not complicate the method due to paralleling. Two examples are considered — a linear oscillator and a Jacobi oscillator with two quadratic integrals. The second example shows that the preservation of one integral of motion does not lead to the conservation of the other. Moreover, this method allows us to propose a practical application of the well-known ambiguity in the definition of Butcher tables.

Key words and phrases: finite difference method, dynamical systems, explicit Runge–Kutta methods

1. Introduction

Many dynamical systems have algebraic integrals of motion [1], but standard numerical methods do not allow preserving these integrals exactly on the approximate solution [2]. This means that the approximate solution satisfies such fundamental laws of nature as the law of conservation of energy also approximately, and, in view of the importance of this law itself, this circumstance is always striking.

Consider the dynamical system

$$\frac{dx}{dt} = f(x), \quad x \in \mathbb{R}^m, \quad (1)$$



whose right side is a rational function with rational coefficients. Since difference schemes are described by algebraic equations, there are no obstacles to the case that among these schemes there be those that preserve all the algebraic integrals of this system. Linear integrals of motion are preserved by almost all schemes used. In the late 1980s, among the Runge–Kutta schemes, a subclass of schemes was discovered that preserves not only linear, but also quadratic integrals of motion. This class is called Runge–Kutta symplectic schemes [2]. These schemes make it possible, for example, to preserve all algebraic integrals in the top rotation problem, with the exception of the Kovalevskaya case [3]. In the 1990s, Greenspan constructed the first difference scheme for the many-body problem that preserves all algebraic integrals of this problem [4–7], using the principle of energy quadratization; such schemes can be constructed for the many-body problem based on any Runge–Kutta symplectic scheme [8, 9].

The main disadvantage of symplectic Runge–Kutta schemes is their implicit nature: in calculations using these schemes, a system of nonlinear equations has to be solved at each step, which significantly complicates the calculations compared to the commonly used explicit schemes. Unfortunately, in any case, there are no such schemes among Runge–Kutta schemes, which became clear at the dawn of the theory of symplectic Runge–Kutta schemes [2].

In the paper by del Buono and Mastroserio [10] an approach to constructing conservative difference schemes was proposed, which can be described as follows. Let the dynamical system (1) have an integral g and let there be two difference schemes. Let the step of the first scheme be described as $\hat{x} = \phi(x, dt)$, and the step of the second scheme as $\hat{x} = \psi(x, dt)$. Consider the composite scheme

$$\hat{x} = \phi(x, dt) + \mu\psi(x, dt).$$

We use the parameter μ in such a way that the given integral g be preserved on the approximate solution found exactly by the composite scheme.

To do this, we will describe the transition from n to $n + 1$ as follows: x_n is given, and the next value x_{n+1} is found from the system of equations

$$x_{n+1} = \phi(x_n, dt) + \mu_{n+1}\psi(x_n, dt), \quad g(x_{n+1}) = g(x_n),$$

whose solution reduces to solving one equation

$$g(\phi(x_n, dt) + \mu_{n+1}\psi(x_n, dt)) = g(x_n)$$

with respect to μ_{n+1} .

Such an approach, of course, does not avoid the main difficulty that arises when using implicit difference schemes: at each step, you still have to solve a nonlinear algebraic equation. But this is only one equation and its degree coincides with the degree of the integral g . Therefore, the pioneers called it the explicit conservative Runge–Kutta method.

In fact, this method certainly does not belong to the Runge–Kutta family of methods. In terms of difference schemes, it can be written as follows. One more variable μ is added to the variables x and the transition from (x, μ) to

$(\hat{x}, \hat{\mu})$ is described by a system of algebraic equations

$$\hat{x} = \phi(x, dt) + \hat{\mu}\psi(x, dt), \quad g(\hat{x}) = g(x).$$

It should be noted that this system is not a difference scheme for any dynamical system in the variables (x, μ) . Here we are dealing with a certain generalization of the very concept of a difference scheme.

In Ref. [11] it was proposed to use as ψ the Runge–Kutta scheme nested in the ϕ scheme and having a smaller order. Such an approach was fully justified then, since it promised to reduce the cost of calculating ψ . However, now that multi-core processors have come into general use, it seems superfluous to impose such a restriction: it is easier to calculate $\phi(x_n, dt)$ and $\psi(x_n, dt)$ at each step in parallel.

In fact, the described approach, which we will call del Buono and Mastroserio approach, makes it possible on the basis of any two explicit difference schemes, including any two explicit Runge–Kutta difference schemes, to construct a new numerical algorithm for integrating a dynamical system that preserves the integral g . There is some arbitrariness [12] when calculating explicit Butcher tables, which give the highest possible order of approximation for a fixed number of stages. Therefore, two Runge–Kutta schemes of the same order, but with different Butcher tables, can be taken as two schemes.

We have implemented del Buono and Mastroserio’s approach in the Sage computer algebra system, and in a series of computer experiments we have seen that it does indeed preserve the integrals of motion [13]. Since then, a number of our developments related to the solution of ordinary differential equations using the finite difference method was compiled into the `fdm` for Sage package presented at ITTMM’2022 [14]. In this article, we want to discuss the details of the implementation of del Buono and Mastroserio’s approach in our package. Since it has built-in tools for working with Butcher tables and estimating the approximation error, we will further evaluate the possibility of using two Runge–Kutta schemes of the same order, but with different Butcher tables. The implementation itself is available at <https://github.com/malykhmd/fdm>.

2. Implementation of del Buono and Mastroserio’s approach

Let a dynamical system (1) be given, its integral of motion g , which will be preserved in the numerical solution, and two explicit Runge–Kutta difference schemes $\hat{x} = \phi(x, dt)$ and $\hat{x} = \psi(x, dt)$, which are given using two Butcher tables. Our implementation of the del Buono and Mastroserio approach in `fdm` for Sage supports any pair of Butcher tables.

With two stages, the highest order of approximation that Runge–Kutta schemes can have is 2. In this case, one parameter of the Butcher table remains undefined. Therefore, in our experiments, schemes with Butcher

tables were taken as two initial schemes

$$\begin{array}{c|cc} 1 & 1 & \\ \hline & \frac{1}{2} & \frac{1}{2} \end{array} \quad \text{and} \quad \begin{array}{c|cc} 2 & 2 & \\ \hline & \frac{3}{4} & \frac{1}{4} \end{array}$$

To calculate an approximate solution of the Cauchy problem

$$\dot{x} = f(x), \quad x|_{t=0} = x_0$$

on the segment $0 < t < T$, we divide this segment into N equal parts with the step $dt = T/N$. Then, in a loop over $n = 1, 2, \dots, N$, we calculate x_1, x_2, \dots . At each step in n , we first calculate the values $x'_{n+1} = \phi(x_n, dt)$ and $x''_{n+1} = \psi(x_n, dt)$ by these schemes in parallel, then we calculate the root of the equation

$$g(x'_{n+1} + \mu x''_{n+1}) = g(x_n) \tag{2}$$

relative to μ . Then we find

$$x_{n+1} = x'_{n+1} + \mu x''_{n+1}.$$

In this case, a certain arbitrariness arises in the choice of the method for solving the algebraic equation (2). When applying implicit Runge–Kutta methods, iterative methods are used, since there is a natural approximation to the desired root [7]. In this case, however, we do not know a good approximation to μ , and the equation itself has a small degree and, at least in the examples considered below, admits a solution in radicals. We tried different methods for solving this equation, in particular, explicitly expresses the solution in radicals, but this did not give any noticeable increase in comparison with the standard method of finding the roots of polynomials $\mathbb{R}[\mu]$, implemented in Sage.

3. Test examples

As a first test case, we took a linear oscillator

$$\begin{cases} \frac{d}{dt}x = y, & \frac{d}{dt}y = -x, \\ x(0) = 0, & y(0) = 1 \end{cases} \tag{3}$$

in the segment $0 < t < 10$.

In figure 1, it is clearly seen that the quadratic integral of motion $x^2 + y^2$ is preserved on the approximate solution found by the composite scheme, which favorably distinguishes this scheme from the usual explicit Runge–Kutta scheme. The slope of the Richardson diagram (figure 2) [15] shows that the order of approximation of the composite circuit is equal to the order of the original ones, that is, 2, as expected from theoretical considerations. It should also be noted that the value of μ did not change from step to step.

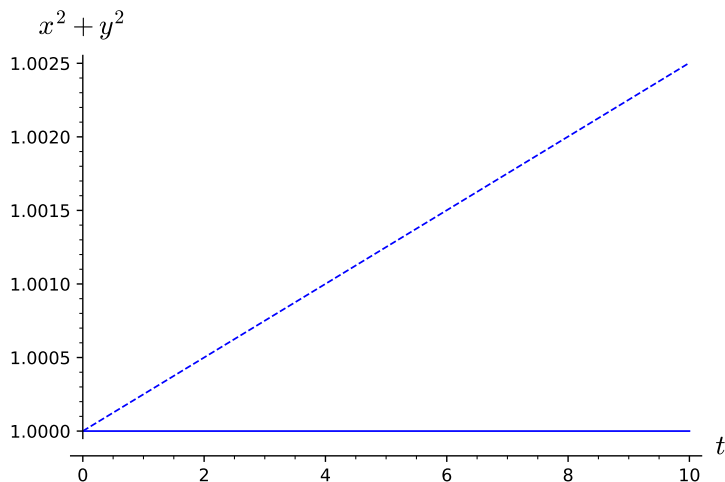


Figure 1. Variation of integral $x^2 + y^2$ on the approximate solutions of the problem (4): the explicit Runge–Kutta scheme (dotted line) and the composite scheme (solid line)

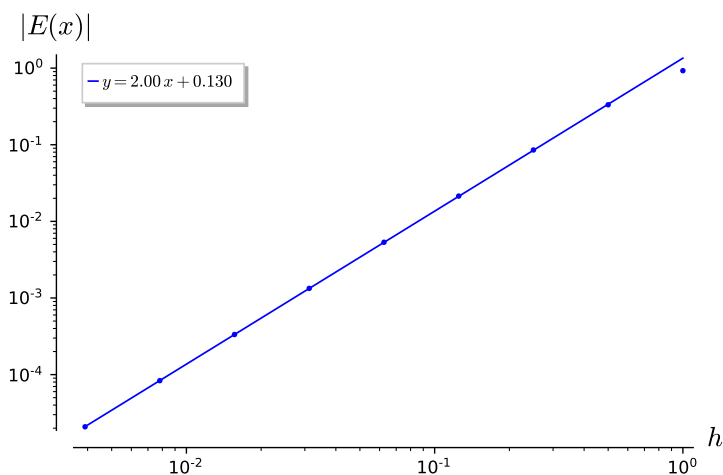


Figure 2. Richardson diagram for the value of x at $t = 9$ in the example (4)

As a second test case, we took the Jacobi oscillator:

$$\begin{cases} \frac{d}{dt}p = qr, & \frac{d}{dt}q = -pr, & \frac{d}{dt}r = -\frac{1}{4}pq, \\ p(0) = 0, & q(0) = 1, & r(0) = 1 \end{cases} \quad (4)$$

in the segment $0 < t < 10$. This system admits two independent quadratic integrals, we took $p^2 + q^2$ as g .

In figure 3, it is clearly seen that this integral of motion $p^2 + q^2$ is preserved on the approximate solution found by the composite scheme. However, the second integral $p^2/4 + r^2$ is not preserved in this case (see figure 4). According

to the Richardson diagram (figure 5), it can be seen that in this case, too, the order of approximation of the composite circuit is equal to that of the original ones. Unlike the linear case, the value of μ changed from step to step, and very smoothly (figure 6).

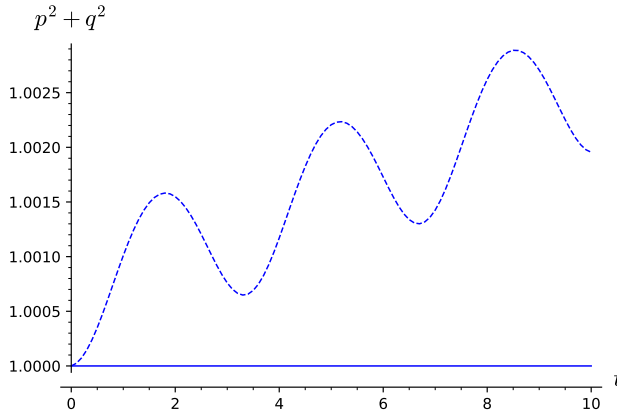


Figure 3. Variation of the integral $x^2 + y^2$ on approximate solutions of the problem (3): explicit Runge-Kutta scheme (dotted line) and composite scheme

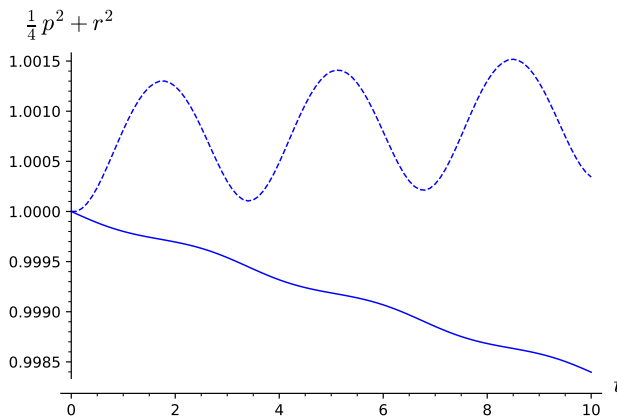


Figure 4. Variation of the integral $x^2 + y^2$ on approximate solutions of the problem (3): explicit Runge-Kutta scheme (dotted line) and composite scheme (solid line)

4. Conclusion

The performed experiments confirm that the approach, which goes back to the article by del Buono and Mastroserio [10], can also be used with a non-standard choice of initial schemes. Moreover, this method allows us to offer a practical application of the well-known ambiguity in the definition of Butcher tables.

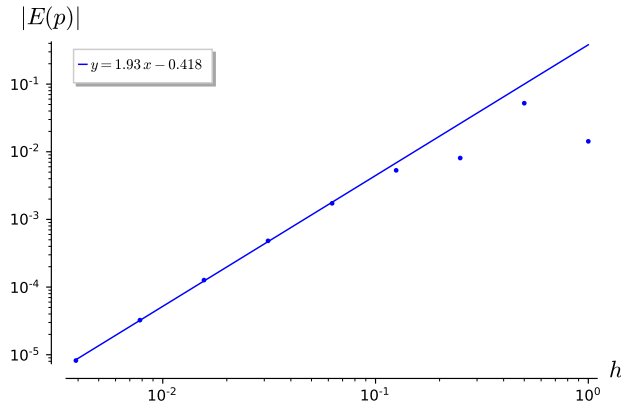


Figure 5. Richardson diagram for value x at $t = 9$ for example (3)

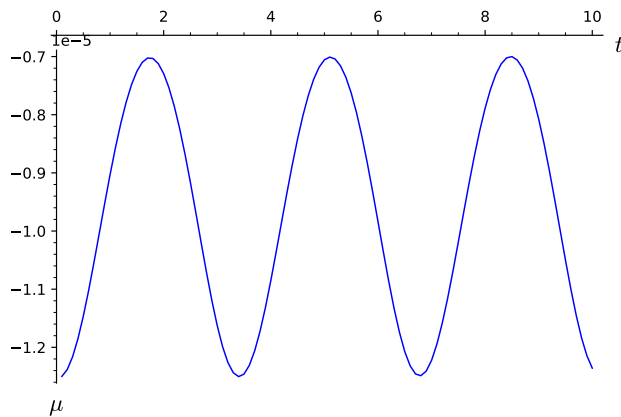


Figure 6. Dependence of parameter μ on time t for example (3)

However, we should admit that the main problem of all known conservative schemes, the necessity to solve nonlinear equations at each step, has not been completely eliminated. The gain that the described method gives can be described as follows. If only one integral of motion of a dynamical system with n unknowns needs to be preserved, the Runge–Kutta symplectic method leads to the solution of a system of n algebraic equations at each step, and the method under discussion only one equation with one unknown. It is well known that numerical methods for solving one equation with one unknown are much simpler and more reliable than methods for solving systems [16]. The smoothness of changing the values of the parameter μ noted above suggests that iterative algorithms, for example, Newton's method, can be used to calculate it.

Unfortunately, as was seen in the second test case, the inheritance of one integral of motion does not entail the inheritance of the second. The del Buono and Mastroserio approach has already been generalized to the case of several integrals of motion [11] and in this case leads to the solution of a system of nonlinear equations at each step with respect to several auxiliary

parameters. Thus, we return to the difficulty typical of the symplectic Runge–Kutta methods. The study of the gain that the del Buono and Mastroserio approach gives, when applied to systems with several algebraic integrals of motion, in comparison with classical implicit methods requires further study.

It is no less interesting how the del Buono and Mastroserio approach will show itself in solving the many-body problem, in which the approach of bodies significantly worsens the convergence of iterative methods used to solve nonlinear systems that arise when using the implicit Runge–Kutta methods.

References

- [1] A. Goriely, *Integrability and Nonintegrability of Dynamical Systems*. Singapore; River Edge, NJ: World Scientific, 2001.
- [2] E. Hairer, G. Wanner, and S. P. Nørsett, *Solving Ordinary Differential Equations I, Nonstiff Problems*, 3rd ed. Springer, 2008. DOI: 10.1007/978-3-540-78862-1.
- [3] V. V. Golubev, *Vorlesungen über Differentialgleichungen im Komplexen*. VEB Deutscher Verlag der Wissenschaften, 1958.
- [4] D. Greenspan. “Completely Conservative and Covariant Numerical Methodology for N-Body Problems With Distance-Dependent Potentials. Technical Report no. 285.” (1992), [Online]. Available: <http://hdl.handle.net/10106/2267>.
- [5] D. Greenspan, “Completely conservative, covariant numerical methodology,” *Computers & Mathematics with Applications*, vol. 29, no. 4, pp. 37–43, 1995. DOI: 10.1016/0898-1221(94)00236-E.
- [6] D. Greenspan, “Completely conservative, covariant numerical solution of systems of ordinary differential equations with applications,” *Rendiconti del Seminario Matematico e Fisico di Milano*, vol. 65, pp. 63–87, 1995. DOI: 10.1007/BF02925253.
- [7] D. Greenspan, *N-Body Problems and Models*. World Scientific, 2004.
- [8] Y. Ying, A. Baddour, V. P. Gerdt, M. Malykh, and L. Sevastianov, “On the quadratization of the integrals for the many-body problem,” *Mathematics*, vol. 9, no. 24, 2021. DOI: 10.3390/math9243208.
- [9] A. Baddour and M. Malykh, “On difference schemes for the many-body problem preserving all algebraic integrals,” *Phys. Part. Nuclei Lett.*, vol. 19, pp. 77–80, 2022. DOI: 10.1134/S1547477122010022.
- [10] N. Del Buono and C. Mastroserio, “Explicit methods based on a class of four stage fourth order Runge–Kutta methods for preserving quadratic laws,” *Journal of Computational and Applied Mathematics*, vol. 140, pp. 231–243, 2002.
- [11] M. Calvo, D. Hernández-Abreu, J. I. Montijano, and L. Rández, “On the preservation of invariants by explicit Runge–Kutta methods,” *SIAM Journal on Scientific Computing*, vol. 28, no. 3, pp. 868–885, 2006.

- [12] Y. Ying, “The symbolic problems associated with Runge-Kutta methods and their solving in Sage,” *Discrete and Continuous Models and Applied Computational Science*, vol. 27, no. 1, pp. 33–41, 2019. DOI: 10.22363/2658-4670-2019-27-1-33-41.
- [13] Y. Ying and M. Malykh, “On the realization of explicit Runge–Kutta schemes preserving quadratic invariants of dynamical systems,” *Discrete and Continuous Models and Applied Computational Science*, vol. 28, no. 4, pp. 313–331, 2020. DOI: 10.22363/2658-4670-2020-28-4-313-331.
- [14] L. González and M. D. Malykh, “On a new package for the numerical solution of ordinary differential equations in Sage,” in *Information and telecommunication technologies and mathematical modeling of high-tech systems. Materials of the All-Russian Conference with international participation*, In Russian, Moscow: RUDN, 2022.
- [15] A. Baddour and M. Malykh, “Richardson–Kalitkin method in abstract description,” *Discrete and Continuous Models and Applied Computational Science*, vol. 29, no. 3, pp. 271–284, 2021.
- [16] W. H. Press. “Numerical Recipes Home Page.” (2019), [Online]. Available: <http://numerical.recipes>.

For citation:

Y. Ying, Z. Lu, Conservative finite difference schemes for dynamical systems, *Discrete and Continuous Models and Applied Computational Science* 30 (4) (2022) 364–373. DOI: 10.22363/2658-4670-2022-30-4-364-373.

Information about the authors:

Ying, Yu — Assistant Professor of Department of Algebra and Geometry, Kaili University, China (e-mail: 45384377@qq.com, ORCID: <https://orcid.org/0000-0002-4105-2566>)

Lu, Zhen — Associate Professor, Department of Fine art, Kaili University, China (e-mail: 157739594@qq.com, ORCID: <https://orcid.org/0000-0002-7526-9026>)

УДК 519.872:519.217

PACS 07.05.Tr, 02.60.Pn, 02.70.Bf

DOI: 10.22363/2658-4670-2022-30-4-364-373

Консервативные конечно-разностные схемы для динамических систем

Юй Ин, Чжэнь Лу

*Университет Кайли,
3, Кайюань Роуд, Кайли, 556011, Китай*

Аннотация. В статье представлена реализация одного из подходов к интегрированию динамических систем, при котором сохраняются алгебраические интегралы в оригинальной системе `fdm for sage`. Этот подход, восходящий к статье дель Буоно и Матросерио, позволяет на основе двух любых явных разностных схем, в том числе любых двух явных схем Рунге–Кутты, сконструировать новый численный алгоритм интегрирования динамической системы, сохраняющий заданный интеграл. Этот подход реализован и протестирован в оригинальной системе `fdm for sage`. Обсуждены детали и трудности реализации. Для тестирования в качестве двух схем взяты две схемы Рунге–Кутты одного порядка, но с разными таблицами Бутчера, что не приводит к усложнению метода благодаря распараллеливанию. Рассмотрено два примера — линейный осциллятор и осциллятор Якоби, имеющий два квадратичных интеграла. На втором примере показано, что сохранение одного интеграла движения не приводит к сохранению другого. Проведенные эксперименты подтверждают, что данный подход может быть использован и при нестандартном выборе исходных схем. Более того, этот метод позволяет предложить практическое применение хорошо известной неоднозначности в определении таблиц Бутчера.

Ключевые слова: метод конечных разностей, динамические системы, явные методы Рунге–Кутты



UDC 533.951.8

DOI: 10.22363/2658-4670-2022-30-4-374-378

Approximation of radial structure of unstable ion-sound modes in rotating magnetized plasma column by eikonal equation

Nikita A. Marusov^{1,2}

¹ Kurchatov Institute,

1, Kurchatov Square, Moscow, 123182, Russian Federation

² Peoples' Friendship University of Russia (RUDN University),
6, Miklukho-Maklaya St., Moscow, 117198, Russian Federation

(received: November 15, 2022; revised: December 12, 2022; accepted: December 19, 2022)

Abstract. The problem of the correct asymptotic construction of the radial structure of linearly unstable ion-sound electrostatic eigenmodes is studied. The eigenvalue problem with boundary conditions of the first and second kind (electrodynamic and hydrodynamic types) for the oscillations that propagate in a uniform cylindrical column of magnetized plasma along an axial homogeneous magnetic field is formulated. A method for constructing a discrete spectrum of small-scale unstable oscillations of the system based on the basic principles of geometric optics is proposed. The main idea of the method is an explicit idea of the type of boundary conditions — the conductivity and absorbing properties of the wall bounding the plasma cylinder. A dispersion relation for unstable small-scale modes destabilized due to the effects of differential rotation is derived from the Eikonal equation. For the correct construction instability growth rates spectra a universal recipe for the selection of radial wave numbers of small-scale eigenmodes in accordance with any of the types of boundary conditions is proposed.

Key words and phrases: plasma waves, plasma instabilities, geometrical optics, normal modes

1. Introduction

It is well known that rotation of the plasmas in magnetic field is a source of various instabilities [1–6]. The most common of them are of a convective nature and occur for non-axisymmetric flute-like perturbations with $m \neq 0$ and $k_{\parallel} = 0$ (m is the azimuthal wave-number of perturbations and k_{\parallel} is the projection of the wave vector on the direction of magnetic field). Recently was shown that electrostatic axisymmetric ($m = 0$) perturbations with frequencies in the ion-sound region in uniform plasma column in homogeneous magnetic field are destabilized by rotation, if the generalized momentum of ions decreases

© Marusov N. A., 2022



This work is licensed under a Creative Commons Attribution 4.0 International License

<https://creativecommons.org/licenses/by-nc/4.0/legalcode>

with radius [7]. However, the question about radial structure of these unstable perturbations is still open.

In this paper we estimate a radial structure of unstable eigenmodes in a differentially rotating magnetized plasma column. Solutions of wave equation for axisymmetric perturbations is obtained by geometrical optics approximation. The corresponding dispersion relation is derived from eikonal equation.

2. Wave equation

The general wave equation for axisymmetric perturbations of the electrostatic potential Φ in a differentially rotating uniform plasma column with cold ions and hot electrons immersed in the axial magnetic field takes the following form, [7]:

$$\frac{1}{r} \left(\frac{c_s^2}{\omega^2 - \kappa(r)\omega_{Bi}^2} r\Phi' \right)' + \left(1 - \frac{k_{\parallel}^2 c_s^2}{\omega^2} \right) \Phi = 0. \tag{1}$$

where c_s is the ion-sound speed, ω is the perturbation frequency, ω_{Bi} is the ion-cyclotron frequency and k_{\parallel} is the wavelength along axial magnetic field. The variable

$$\kappa(r) = \left(1 + 2\frac{\Omega}{\omega_{Bi}} \right) \left(1 + \frac{1}{r} \frac{(r^2\Omega)'}{\omega_{Bi}} \right) \tag{2}$$

defines the rotation profile of plasma Ω . Prime implies the radial derivative $d(\dots)/dr$. Without rotation, $\Omega = 0$, Eq. (1) describes propagation of the ion-sound waves along cylindrical plasma waveguide.

Together with the boundary conditions (BC), Eq. (1) constitutes the eigenvalue problem. At the center of plasma column, $r = 0$, the solution is required to be finite, $|\Phi(0)| < \infty$. On the inner wall there are two types of BCs exist. For plasma column with ideally conducting wall at radius R , we require $\Phi(r = R) = 0$, which provides zero tangential component of the perturbed electric field, $\tilde{E}_z = -k_{\parallel}\Phi$. If the inner wall does not absorb particles, we require $\Phi'(r = R) = 0$ that corresponds the standard “no flux” BC in fluid dynamics, because displacement of ions is proportional to radial electric field $\tilde{E}_r = -\Phi'$ [7, 8].

3. Solution of eikonal equation for unstable perturbations

For an arbitrary profile of rotation $\Omega(r)$ the exact solution of the Eq. (1) does not exist. However, the studied problem can be solved asymptotically. At first, let us consider solution of the Eq. (1) in the following form

$$\Phi(r) = A(k, S(r)) \exp[ikS(r)], \tag{3}$$

where k is the radial wavenumber and $S(r)$ is the eikonal [9, 10]. In the lowest order by $1/k$ one can find the standard eikonal equation

$$(S')^2 = N^2. \quad (4)$$

Here N is the refractive index of the medium, which is in considered problem equals

$$k^2 N^2(r) = - \left(1 - \frac{k_{\parallel}^2 c_s^2}{\omega^2} \right) \left(\frac{\omega^2 - \kappa(r) \omega_{Bi}^2}{c_s^2} \right). \quad (5)$$

As easily seen, the instability occurs only when $\kappa(r) < 0$. For unstable solutions with growth rate $\gamma = -i\omega$ Eq. (5) gives

$$\hat{N}^2(r) = \left(1 + \frac{k_{\parallel}^2 c_s^2}{\gamma^2} \right) \left(\frac{\gamma^2 - |\kappa(r)| \omega_{Bi}^2}{k^2 c_s^2} \right) \geq 0 \quad (6)$$

and Eq. (3) have only one trivial solution

$$S(r) = \int_0^r \hat{N}^2(x) dx. \quad (7)$$

Finally, the desired solution of the wave equation (1) in the lowest order of geometrical optics approximation takes the form

$$\Phi(r, z, t) = \Phi_0 \exp \left[ik \int_0^r \hat{N}^2(x) dx \right] \exp [i(k_{\parallel} z - \omega t)], \quad (8)$$

where Φ_0 is the complex amplitude.

Thus, one can find that Eq. (8) could be used for construct eigenfunctions with discrete spectra of γ_n by discrete values of radial wavenumbers $n = \pi/kR$:

$$\begin{aligned} \Phi_n(r, z, t) = \Phi_0 \left\{ \cos \left[k \int_0^r \hat{N}_n^2(x, \gamma_n) dx \right] + i \sin \left[k \int_0^r \hat{N}_n^2(x, \gamma_n) dx \right] \right\} \times \\ \times \exp [i(k_{\parallel} z - \omega t)]. \quad (9) \end{aligned}$$

4. Conclusion

It is shown that a sufficiently complex wave equation (1) for the electrostatic ion-sound perturbation of magnetized plasma with an arbitrary profile of rotation can be solved analytically by the geometrical optics approximation. The radial structure of normal modes is constructed by Eq. (9) and their spectra are described by eikonal (7).

References

- [1] A. B. Mikhailovskii, *Theory of plasma instabilities: Volume 1: Instabilities of a homogeneous plasma*. New York: Consultants Bureau, 1974.
- [2] A. B. Mikhailovskii, *Theory of plasma instabilities: Volume 2: Instabilities of a homogeneous plasma*. New York: Consultants Bureau, 1974.
- [3] E. P. Vedenov, R. Z. Velikhov, and R. Z. Zagdeev, “Stability of plasma,” *Sov. Phys. Usp.*, vol. 4, pp. 332–369, 1961.
- [4] A. V. Timofeev, “Oscillations of inhomogeneous flows of plasma and liquids,” *Sov. Phys. Usp.*, vol. 13, pp. 632–646, 1971.
- [5] A. B. Mikhailovskii *et al.*, “High-frequency extensions of magnetorotational instability in astrophysical plasmas,” *Plasma Physics Reports*, vol. 34, no. 8, pp. 678–687, 2008.
- [6] D. A. Shalybkov, “Hydrodynamic and hydromagnetic stability of the couette flow,” *Physics-Uspokhi*, vol. 52, no. 9, pp. 915–935, 2009.
- [7] N. A. Marusov *et al.*, “Stability of electrostatic axisymmetric perturbations in rotating Hall plasmas,” in *Proc. 47th EPS Conference on Plasma Physics*, EPS 2021, Sitges, Spain, 2021, p. 16 190.
- [8] L. D. Landau and E. M. Lifshitz, *Fluid Mechanics. Course of Theoretical Physics. Vol. 6*. New York: Pergamon Press, 1987.
- [9] S. Borowitz, *Fundamentals of quantum mechanics: Particles, waves, and wave mechanics*. New York: Pergamon Press, 1967.
- [10] A. V. Timofeev, “Geometrical optics and the diffraction phenomenon,” *Phys. Usp.*, vol. 48, pp. 609–613, 2005.

For citation:

N. A. Marusov, Approximation of radial structure of unstable ion-sound modes in rotating magnetized plasma column by eikonal equation, *Discrete and Continuous Models and Applied Computational Science* 30 (4) (2022) 374–378. DOI: 10.22363/2658-4670-2022-30-4-374-378.

Information about the authors:

Marusov, Nikita A. — Candidate of Sciences in Physics and Mathematics, Senior Researcher of Department of Plasma Theory of Kurchatov Institute; Senior Lecturer of Institute of Physical Research and Technology of Peoples’ Friendship University of Russia (RUDN University) (e-mail: marusov-na@rudn.ru, phone: +7(499) 196-77-03, ORCID: <https://orcid.org/0000-0002-0763-1505>)

УДК 533.951.8

DOI: 10.22363/2658-4670-2022-30-4-374-378

Построение радиальной структуры неустойчивых ионно-звуковых колебаний во вращающейся замагниченной плазме при помощи уравнения эйконала

Н. А. Марусов^{1,2}

¹ *Научно-исследовательский центр «Курчатовский институт»,
пл. Академика Курчатова, д. 1, Москва, 123182, Россия*

² *Российский университет дружбы народов,
ул. Миклухо-Маклая, д. 6, Москва, 117198, Россия*

Аннотация. Рассмотрена задача о корректном асимптотическом построении радиальной структуры линейно неустойчивых собственных электростатических колебаний ионно-звукового типа, распространяющихся в однородном цилиндрическом столбе замагниченной плазмы вдоль осевого однородного магнитного поля. В цилиндрической области пространства координат сформулирована задача на собственные значения с краевыми условиями первого и второго рода (электродинамического и гидродинамического типа) для волнового уравнения ионно-звуковых колебаний. На основе базовых принципов геометрической оптики предложен метод построения дискретного спектра мелкомасштабных неустойчивых колебаний исследуемой системы, в основе которого лежит явное представление о типе краевых условий — проводимости и поглощающих свойствах стенки, ограничивающей плазменный цилиндр. При помощи уравнения эйконала получено дисперсионное соотношение для неустойчивых собственных мелкомасштабных мод, дестабилизированных за счёт эффектов дифференциального вращения — неоднородного по радиусу профиля угловой скорости ионов, вращающихся вокруг оси симметрии, вдоль которой направлен вектор индукции магнитного поля. Для корректного построения спектра дискретных инкрементов неустойчивых колебаний предложен универсальный рецепт подбора радиальных волновых чисел мелкомасштабных собственных мод в соответствии с каким-либо из типов краевых условий.

Ключевые слова: волны в плазме, неустойчивости плазмы, геометрическая оптика, собственные колебания